Deep structure of the Demerara Plateau and its two-fold tectonic evolution: from a volcanic margin to a Transform Marginal Plateau, insights from the conjugate Guinea Plateau

David Graindorge, Thomas Museur, Frauke Klingelhoefer, Walter Roest, Christophe Basile, Lies Loncke, François Sapin, Arnaud Heuret, Julie Perrot, B. Marcaillou, et al.

Accepted Manuscript

Geological Society, London, Special Publications

Deep structure of the Demerara Plateau and its two-fold tectonic evolution: from a volcanic margin to a Transform Marginal Plateau, insights from the conjugate Guinea Plateau

D. Graindorge, T. Museur, F. Klingelhoefer, W. R. Roest, C. Basile, L. Loncke, F. Sapin, A. Heuret, J. Perrot, B. Marcaillou, J-F Lebrun & J. Déverchère

DOI: https://doi.org/10.1144/SP524-2021-96

To access the most recent version of this article, please click the DOI URL in the line above. When citing this article please include the above DOI.

Received 1 June 2021
Revised 9 February 2022
Accepted 11 February 2022

Deep structure of the Demerara Plateau and its two-fold tectonic evolution: from a volcanic margin to a Transform Marginal Plateau, insights from the conjugate Guinea Plateau

D. Graindorge[1], T. Museur[1,2], F. Klingelhoefer[2], W. R. Roest[2], C. Basile[3], L. Loncke[4], F. Sapin[5], A. Heuret[6], J. Perrot[1], B. Marcaillou[7], J-F., Lebrun[8] and J. Déverchère[1]

1. University of Brest, CNRS, IUEM, Plouzané, France, david.graindorge@univ-brest.fr
2. Ifremer, Centre de Brest, UR Géosciences Marines, BP 70, 29280 Plouzané, France
3. ISTerre, UMR-CNRS 5275, Observatoire des Sciences de l'Univers de Grenoble, Université Joseph Fourier, Maison des Géosciences, 1381 rue de la Piscine, 38400 St. Martin d'Hères, France
4. University of Perpignan Via Domitia, Centre de Formation et de Recherche sur les Environnements Méditerranéens (CEFREM), UMR 5110, 52 Avenue Paul Alduy, 66100, Perpignan, France
5. Total SA, Centre Scientifique et Technique Jean Feger (CSTJF), Avenue Larribau, 64018, Pau, France
6. Université de Guyane, Géosciences Montpellier, Université de Montpellier, CNRS Université des Antilles, Cayenne, Guyane.
7. University Côte d'Azur, CNRS, Observatoire de la Côte d'Azur, IRD, Géoazur, Valbonne, France
8. Géosciences Montpellier, Université de Montpellier, CNRS, Université des Antilles, Pointe à Pitre, Guadeloupe (FWI)

Abstract

Transform marginal Plateaus (TMPs) are large and flat structures commonly found in deep oceanic domains, but origin and relationship to adjacent oceanic lithosphere remain poorly understood. This paper focuses on two conjugate TMPs, the Demerara Plateau off Suriname and French Guiana and the Guinea Plateau, located at the junction of the Jurassic Central Atlantic and the Cretaceous Equatorial Atlantic Oceans. The study helps to understand (1) the tectonic history of both Demerara and Guinea Plateaus, (2) the relationship between the Demerara Plateau and the adjacent oceanic domains and finally, (3) to throw light on the formation of Transform Marginal Plateaus (TMPs). We analyze two existing wide-angle seismic derived velocity models from the MARGATS seismic experiment (Demerara Plateau), and adjacent composite industrial seismic lines covering the Demerara and Guinea Plateaus. The Demerara Plateau displays a 30 km thick crust, subdivided into 3 layers, including a high velocity lower crust (HVLC). The velocities and velocity gradients do not fit values of typical continental crust but instead correspond to volcanic margin or Large Igneous Province (LIP) type crusts. We propose that the, possibly continental, lower crust is intruded by magmatic material and that the upper crustal layer is made of extrusive volcanic rocks of the same magmatic origin, forming thick seaward (westward) dipping reflectors (SDRs) sequences. This SDR complex extends to the Guinea Plateau as well and was emplaced during hotspot (Sierra Leone)-related volcanic rifting preceding the Jurassic opening of the Central Atlantic and forming the western margin of the plateau. N-S composite lines linking Demerara and Guinea plateaus reveal the spatial extent of the SDR complex but also a preexisting basement ridge separating the two plateaus. The entire Demerara-Guinea margin would therefore be an inherited Jurassic volcanic margin bordering the Central Atlantic Ocean to the east, with as a possible conjugate being the Bahamas Plateau on the other side of the ocean. This margin was then reworked during a non-coaxial Cretaceous second phase of rifting potentially accompanied by a magmatic event. Opening of the northern margin occurs in a transform mode splitting the Jurassic volcanic margin in two parts (Guinea and Demerara TMPs), conceivably along a pre-

existing basement ridge. Rifting of the eastern part of the Demerara Plateau occurred surprisingly along the eastern limit of the Jurassic SDR complex, forming the present-day eastern divergent margin of the Demerara Plateau. After that stage, the Demerara and Guinea plateaus are individualized on each side of the Equatorial Atlantic. This study also highlights the major contribution of thermal anomalies related to hotspots and superposed tectonic phases in the case of other TMPs which share numerous characteristics with the Demerara Plateau.

Introduction

Marginal plateaus have been recognized as submarine seafloor highs with a flat (or sub-horizontal) top and located clearly deeper than the standard shelf break within the continental slope (Mercier de Lépinay et al., 2016). Most of them are located at the junction between two oceanic domains of different ages (Mercier de Lepinay et al., 2016). For those bordered by at least one transform or oblique margin, Loncke et al. (2020) define the sub-category of Transform Marginal Plateaus (TMPs). As most of these plateaus are associated with at least one major magmatic event (Loncke et al., 2020), TMPs have possibly recorded polyphase tectonic and magmatic histories. Therefore, they provide geodynamic records that may help to better understand complex ocean opening processes, break-up conditions, and the thermomechanical evolution of continental margins at the junction between divergent and transform margins.

Located on each side of the Equatorial Atlantic, the Demerara and Guinea Plateaus are both TMPs corresponding to conjugated transform margins. The Demerara/Guinea TMPs formed at the southern tip of the Jurassic Central Atlantic Ocean and later separated and individualized in a transform mode during the highly oblique Cretaceous (Aptian-Albian) Equatorial Atlantic gateway opening (Nemčok et al., 2015). Different spreading vectors of the Central and Equatorial Atlantics required a development of the Accommodation Block, its role was to accommodate for about 20° mismatch between the Central and Equatorial Atlantic spreading vectors, which decreased from late Aptian-Albian to Paleocene down to 0° (Nemčok et al., 2015).

Across the Demerara Plateau (Figure 1), several academic and industrial data sets have been acquired over the past 20 years which makes it one of the most imaged TMPs. Even if the surface and shallow sub-surface of the plateau had been intensively investigated (Gouyet, 1988; Campan, 1995; Greenroyd et al., 2007; Basile et al., 2013; Pattier et al., 2013; 2015; Loncke et al., 2009, 2016; Mercier de Lépinay, 2016; Tallobre et al., 2016; Fanget et al. 2020), the deeper part of the plateau, located under a thick sedimentary cover was until recently (Nemčok et al., 2015; Reuber et al., 2016; Zinecker, 2020; Casson et al. 2021; Museur et al., 2021) studied less. The Guinea TMP has been less well investigated but recent results are reported in: 1) Olyphant et al. (2017): the southern Guinea Plateau and adjacent margin; Zinecker (2020): a new comparison of Demerara and Guinea Plateaus structure and stratigraphy and Casson et al. (2021): high resolution stratigraphic framework of post-rift evolution of the Demerara Plateau.

In this review paper, we use a combination of wide-angle seismic derived velocity models, industrial seismic multi-channel data and line drawings of seismic lines, mainly based on a recent thesis (Museur, 2020). We depict the state of the art of our knowledge of the deep crustal structure and nature of the Demerara Plateau and their continuity with the Guinea Plateau. These results allow to discuss the possible role of crustal inheritance, thermal anomalies and superposed tectonic phases in formation of TMPs by the comparison with other TMPs and volcanic margins, which share numerous characteristics with the Demerara Plateau. Finally, we propose a simplified two-fold tectonic evolution scheme for both TMPs over time.

1. Geological context

1.1. Origin of TMPs

The Demerara and Guinea conjugate TMPs (Figure 1) have been identified as conjugate TMPs among about twenty marginal plateaus (Loncke et al., 2020) worldwide. TMPs often share a complex tectonic history since they frequently combine different rifting phases and distinct

magmatic events. So far, many different geological processes have been proposed to explain the evolution of TMPs. Some of them result from a hotspot-influenced evolution comparable to Volcanic Passive Margins (VPM) such as the Walvis Ridge in the South Atlantic (Chauvet et al., 2020). Similarly, the Falklands-Malvinas TMP underwent a volcanic episode during its Lower Jurassic break-up in association with the Karoo hotspot province (Barker, 1999; Schimschal & Jokat, 2018, 2019), while the second phase of opening in the Lower Cretaceous led to the creation of the largest transform margin in the world (Loncke et al., 2020). In the northern North Atlantic, the Hatton-Rockall TMP underwent a phase of volcanic underplating (Klingelhoefer et al, 2005; White et al., 2008, White & Smith, 2009,) and/or the development of a volcanic margin (Welford et al., 2012) during its second opening phase. On the other hand, other TMPs remain poorly known partly due to their inaccessibility (e.g. the Gunnerus Ridge: Leitchenkov et al., 2008).

1.2. Kinematic reconstructions

The Demerara and Guinea conjugate TMPs result from a two-fold breakup history. First, the western Demerara and Guinea margins formed during the Jurassic Central Atlantic ocean opening; later, the Demerara and Guinea TMPs separated by transform motion related to the highly oblique Cretaceous opening of the Equatorial Atlantic ocean (Klitgord & Schouten, 1986; Benkhelil et al., 1995; Campan, 1995; Labails et al., 2010; Moulin et al., 2010; Nemčok et al., 2015; Reuber et al., 2016).

Prior to the opening of the Central Atlantic Ocean, the Guyana shield, a vast province extending from Venezuela to Amapá (mostly composed of rocks emplaced during the Trans-Amazonian orogeny between 2.26 and 1.95 My in Paleoproterozoic times), was the western extension of the Western Africa craton within Gondwana. It is worth noting that the opening of the Central Atlantic Ocean was predated by a major magmatic episode corresponding to the Central Atlantic Magmatic Province (CAMP; Marzoli et al., 1999). It is a region of intense magmatic activity dated at 200 My, extending over 2.5 million square kilometers and expressed in Guyana and Guinea by dense networks of doleritic dykes

Later, the opening of the Central Atlantic separates North America and Africa approximately following the Hercynian orogeny from the Newfoundland fracture zone in the north (south of Grand Banks to the west, south of Iberia to the east) to Guyana-Suriname in the south (Klitgord et Schouten, 1986), and was characterized by a NW-SE (Figure 2) opening direction (Nemčok et al., 2015). At 170 My, after rifting, the Guinea and Demerara Plateaus formed the eastern divergent margin of the southern Central Atlantic ocean (Figure 2) facing the Bahamas platform and the Blake Plateau to the North (Pindell and Kennan, 2009). It is precisely this phase that led to the formation of the western continental margin of the Demerara Plateau along the eastern side of the Guyana Basin (Labails et al., 2010; Nemčok et al., 2015) (Figure 2), which corresponds to a small piece of the Jurassic Atlantic Ocean preserved from subduction below the Antilles.

According to Pindell & Kennan (2009), the Guyana Basin and the proto-Caribbean seaway were shifted by a major transform zone (the Guyana Transform). At 124 My (Figure 2), the North American, South American and Northwest African plates formed a triple junction at the transition from the Central Atlantic to the Equatorial Atlantic tectonic phases (Pindell & Kennan, 2009; Campan, 1995; Labails et al., 2010). Later (e.g. 104 My, Figure 2), the triple

junction allowed the connection between the Central Atlantic, a proto Caribbean domain already connected to the Central Atlantic at Jurassic times, and the newly opened Equatorial Atlantic gateway (Pindell & Kennan, 2009). Splitting between the Guinea and Demerara Plateaus results from the opening of this new Cretaceous oceanic domain (Figure 2, 104 My) possibly following the trace of Panafrican orogeny suture (Villeneuve & Cornée, 1994).

The Equatorial Atlantic rifting and early seafloor spreading occurred during the Early Barremian to Aptian (Basile et al., 2005) and extending into Albian (Sapin et al., 2016; Mercier de Lepinay et al., 2016; Olyphant et al., 2017) in a complex oblique mode, connecting the laterally shifted Central Atlantic and South Atlantic oceanic domains (Figure 1), with a change of the opening direction (Campan, 1995). Demerara and Guinea plateaus initially slid apart in a dextral transform mode when the first oceanic crust is proposed to have formed during the late Aptian (circa 115 My) (Basile et al., 2005). Later, at 105 My, a slight modification in the oceanic opening direction may have resulted in the oblique separation of Demerara and Guinea plateaus and would explain why from that time oceanic transform zones are slightly oblique to the Demerara and Guinea transform margins (Campan, 1995; Basile et al., 2013; Nemčok et al., 2015; Reuber et al., 2016) (Figure 2). On the contrary, our latest vertical gravity maps (work in progress) tend to show that the real transform segments of the Demerara Plateau are completely parallel to fracture zones further east.

1.3. The Demerara Plateau

The Demerara TMP is a 230 km long, 170 km wide submarine high off French Guiana and Suriname continental shelves (Figure 1). Previous investigations include seismic surveys and multibeam bathymetry (Gouyet, 1988; Loncke et al., 2009; Basile et al., 2013; Pattier et al., 2013, 2015; Loncke et al., 2016; Sapin et al., 2016; Fanget et al., 2020) but also wide-angle seismics (Greenroyd et al., 2007, 2008; Museur et al., 2021) and ODP drilling (Erbacher et al., 2004; Mosher et al., 2007).

Nowadays, the Demerara TMP exhibits three margins (Figure 1): (1) its western border corresponds to a Jurassic divergent margin, (2) its northern border corresponds to a Cretaceous transform margin, and (3) its eastern border to a Cretaceous divergent margin (Gouyet, 1988; Basile et al., 2013; Nemčok et al., 2015; Sapin et al., 2016; Museur et al., 2021).

Superficial structures include series of stacked Mass Transport Deposits (MTDs) or deep-seated collapses along the plateau that have recorded a history of large-scale slope failures (Loncke et al., 2009; Pattier et al., 2013, 2015) resulting from the combination of the fluid overpressure, the internal geometry of the margin, the presence of a steep transform margin, suitable décollement rheologies at various stratigraphic levels (Pattier et al., 2015), and, at least, since Miocene, the action of deep bottom thermohaline currents regularly eroding the slope (Fanget et al., 2020).

Within the plateau, Gouyet (1988), Benkhelil et al. (1995), Basile et al.(2013), and Mercier de Lépinay, 2016 described the Cretaceous deformation mainly as characterized by E-W to WNW-ESE trending folds related to wrench-related deformations due to a period of transpression dated latest Aptian/early Albian, and sealed and peneplained by a regional and prominent unconformity from the Upper Albian (Gouyet, 1988, Erbacher et al., 2004 and Basile et al.,2013). The narrow continent to ocean transition of the eastern margin (Sapin et al., 2016) is formed by a few tilted blocks with thick fan-shaped Aptian to Mid-Albian syn-rift deposits.

Subsequently, the breakup unconformity is proposed to be Mid-Albian in age (~104 My) and correlates laterally with the major sub-aerial environment related to the Upper Albian unconformity mentioned above. Post-Albian sediments are 4 km thick below the continental shelf and progressively thin towards the northern outer edge of the Demerara Plateau, forming a thick prograding wedge.

The northern slope of the plateau, corresponding to the transform margin, provides a natural cross section through the deeper part of the plateau, outcropping at the seafloor. Along this border, dredges of DRADEM cruise (Basile et al., 2017) have recovered magmatic rocks: basalts, rhyolites (dated to 173.4 ± 1.6 My i.e. Basile et al., 2020), trachy-basalts and basaltic trachy-andesites. All samples share similar trace element composition (Basile et al., 2020). They are Light Rare-Earth Element-enriched, and contain positive anomalies in Nb, Ta, Zr and Hf, typical of ocean island basalts (OIB), and thus indicate a possibly hotspot-related magmatic event supporting the volcanic origin of a part of the plateau (Reuber et al., 2016).

The deep structure of the Demerara Plateau was first imaged by wide-angle seismic data, along a 500 km SSW-NNE oriented line (Greenroyd et al., 2007, 2008) which enabled the Demerara Plateau to be interpreted as a sliver of continental crust thinned during the opening of the Central Atlantic and later reworked orthogonally by the transform Equatorial Atlantic opening. The Demerara Plateau was also imaged by industrial deep-penetrating reflection seismic lines, which unequivocally revealed the existence of very thick and wide Seaward Dipping Reflector (SDR) packages thickening towards the Jurassic Central Atlantic domain (Reuber et al., 2016). To the west below the SDRs Reuber et al. (2016) proposed the existence of an enigmatic "volcanic igneous crust" formed by magmatic processes during the Jurassic opening in relation to the SDR wedges formation. Alternatively, in particular to the east, this might also represent a geological unit pre-dating the opening of the Central Atlantic and including a basement composed in part of meta-sediments corresponding to the Guiana Shield (Precambrian craton) (Mercier de Lépinay et al., 2016). A second set of data from better resolved wide-angle and reflection seismic experiments confirmed this observation and documented a 30 km thick crust under the Demerara Plateau with velocities fitting those of a LIP (Large Igneous Province)-type crust (Museur et al., 2021). Nemčok et al. (2015), Reuber et al (2016) and Museur et al. (2021) proposed that the the Demerara Plateau is part of an inherited Jurassic volcanic margin bordering the southern end of the Central Atlantic Ocean, which may have resulted from the Sierra Leone hotspot activity localized in the Demerara area at the end of the Lower Jurassic (Basile et al., 2020).

1.4. The Guinea Plateau

The less investigated Guinea TMP (Figure 1) is a 220 km long, 120 km semi-circular submarine high off Guinea-Bissau and Guinea. Nowadays the Guinea TMP exhibits two margins (Figure 1): (1) its western border corresponding to a divergent Jurassic margin related to the Central Atlantic ocean opening, (2) its southern border corresponding to a Cretaceous transform margin related to the Equatorial Atlantic ocean opening (Figure 2). Because of this location, the Mesozoic structure and stratigraphy of the Guinea Plateau recorded the combined effects of an older Triassic-Jurassic rift event related to the opening of the Central Atlantic ocean and a younger period of Aptian right-lateral shearing along the Guinea fracture zone during the oblique opening of the Equatorial Atlantic ocean (Klitgord & Schouten, 1986; Benkhelil et al., 1995; Basile et al., 2013; Olyphant et al., 2017) (Figure 2).

Comprehensive geophysical studies of the entire Guinea Plateau are very recent (Olyphant et al., 2017; Zinecker, 2020). Older works resulted in the seismic refraction data over the south and western Guinea Plateau (Sheridan et al., 1969) and magnetic and shallow reflection seismic data (McMaster et al., 1970). Mascle et al. (1986) presented an updated bathymetric map of the Guinea margin showing the contrasting morphologies of slopes. Based on the analysis of seismic data acquired in the eighties, Marinho et al. (1988) and Benkhelil et al. (1995) expanded the Mascle et al. (1986) study and defined two tectonic events affecting the southern Guinea Plateau: 1) rift-related normal faults affecting the Albian and older sequences, and 2) folding, reverse faulting, and transcurrent faulting of Late Cretaceous and older sequences that recorded structural inversion. This inversion was followed by Cenozoic magmatism responsible for the emplacement of numerous volcanoes located immediately south of the plateau and along the transform border. Subsequently, Benkhelil et al. (1995) proposed a schematic reconstruction of the relative location and tectonic evolution of the Demerara and Guinea TMPs by comparing their observations with those of Gouyet (1988).

The Guinea Plateau has been sporadically the object of hydrocarbon exploration since the 1960's, and hydrocarbon discoveries in the early 2000's along the passive margins adjacent to the Guinea Plateau and the Demerara Rise have led to renewed exploration activity (Sayers & Cooke, 2018). Based on recent 2D and 3D seismic datasets and drills acquired on the southern Guinea Plateau and the Sierra Leone margin, Olyphant et al., 2017 show that volcanics and basalts are widespread along the transform to divergent corner off Guinea and Liberia. Their age is mainly Albian but early Aptian basalts have also been drilled. These emplace mainly in relation with Aptian to Albian rifted tilted blocks. Olyphant et al. (2017) emphasize the asymmetry of rifting between Demerara and Guinea areas.

2. Published data

Data synthesized in this paper stem from two datasets. Firstly, academic deep penetrating multichannel reflection and wide-angle seismic data from the Demerara Plateau acquired during the MARGATS (IUEM/Ifremer) oceanographic experiment on the R/V L'Atalante in 2016 were modeled and interpreted (Museur et al., 2021). Secondly, a dataset of industrial Multi-Channel Seismic (MCS) lines including several sets of deep-penetrating reflection seismic data, some of them imaging down to 16 s (TWT), covering the Demerara and Guinea Plateaus.

During the MARGATS experiment, 80 ocean-bottom seismometers (OBS) were used for 171 deployments. They were deployed along four combined reflection and wide-angle seismic profiles, two of which are discussed in this study (Figure 1). We used a 6500 cubic inch airgun array seismic source fired every 60 seconds corresponding to a 150 m shot spacing. In this paper we present two-way time converted velocity models from the eastern part of the Plateau (Figure 2) derived from wide-angle seismic and coincident academic MCS for comparison with industrial MCS data (Figures 3 and 4): the NE-SW MAR01 (56 OBS) profile crossing the eastern divergent margin at its intersection with the northern transform margin and the WNW-ENE MAR02 (37 OBS) profile intersecting the eastern divergent margin. Coincident MCS Margats data are used to control geometries of upper layers. They were pre-processed on board using the *SolidQC* software from Ifremer and processing was completed in the laboratory using either *Geovation* software (CGG) or SeisSpace ProMax. The processing included filtering, deconvolution, NMO correction, stacking, velocity analysis, and time migration. Detailed analysis and presentation of the wide-angle data can be found in Museur et al. (2021). Wide-

angle data were modeled using the RAYINVR forward modeling software (Zelt & Smith, 1992). The superficial layers (from the seafloor down to the top of the crust) were further constrained by bathymetric data and the coincident MCS data. We used a minimum structure/parameter approach to avoid inclusion of structures unconstrained by the data and gravity modeling to test the broad structure of the velocity models. Details of modelling processes, error estimation and coincident gravity modeling used to verify and extend the seismic models are presented in Museur et al. (2021).

Combined line drawings from the Demerara Plateau presented in this paper result from interpretation of industrial MCS data including (Figure 1): 1) ION Geophysical GuyanaSPAN 2D seismic survey. The survey images the plateau and its margins in water depths of 40-3500 m and was provided by TOTAL SA in two-way travel time (TWT) cut at 16 seconds. Pre-stack depth converted sections were published in Reuber et al. (2016) and Casson et al., 2021). 2) CGG MCS correspond to high quality 8 seconds data in TWT covering the western Demerara Plateau. 3) Fugro seismic data set is composed of 5 km spaced 12 s (TWT) lines covering the eastern part of the plateau and margin.

The age and nature of the different units is partially constrained by well data (Mercier et al., 2016) and includes the Sinnamary, FG-2 and Demerara A2 wells (Figure 1). Sinnamary (SE Demerara) penetrates post-Albian to Lower Cretaceous sedimentary series, which are mainly composed of sands and claystones down to an undated basement gneiss proposed to correspond to French Guianese Precambrian. The FG-2 well (eastern Demerara) drilled through Post-Albian series, the Albian unconformity, Aptian to Neocomian sediments down to Barremian basalts intercalated with sands (Gouyet, 1988). The Demerara A2 well (western plateau) penetrates post-Albian claystones and carbonates, the Albian unconformity down to shallow water claystones and carbonates proposed to be either Aptian and Neocomian for the claystones and a Jurassic age (Oxfordian) for the carbonates (Gouyet, 1988; Loncke et al., 2020), or Callovian for the carbonates from alternative biostratigraphic interpretations (Nemčok et al., 2015; Griffith, 2017). However, a more recent study (Casson et al., 2021) proposes an age no older than late Tithonian based on calpionellid occurrence. In this study, we consider that they correspond to a carbonate platform developed along the Central Atlantic Demerara margin from late Jurassic to Neocomian.

The shelf, slope and deepwater areas of the Guinea Plateau, varying between 10 m to 4800 m water depth, have been mainly covered by TGS seismic surveys (2012, 2017), although these data are not as good quality as the GXT lines. TGS lines were available (courtesy TOTAL SA) down to 9 or 14 seconds TWT. The Continent Ocean Boundary is poorly imaged. Some of these lines are shown in pre-stack depth migrated format in Zinecker (2020) and Casson et al. (2021).

Overall, the combination of velocity and geometry of the layers allows a robust interpretation and is used to propose the chronology and processes that led to the formation of Demerara and Guinea plateaus.

3. Results and synthesis

3.1. The Demerara Plateau

Velocity models

We focus on the velocity distribution of model MAR01 (Figure 5a) because MAR01 and MAR02 (see Figure 1 for location) models show relatively similar structural patterns. Detailed results and data can be found in Museur et al. (2021). Nevertheless, both models are presented as two-way time-converted along composite lines D2 and D3 (Figures 3 and 4). The MAR01 model is composed of seven layers including: the water column, two sedimentary layers, three underlying crustal layers, and the mantle layer. According to lateral variations in layer thicknesses and velocity-depth laws (Figure 5), model was divided into three parts: plateau, transition and ocean domains (Figure 5). Based on velocities and gradients within the plateau domain, the 25 km thick deep crust can be divided into three layers: upper crust, middle crust and lower crust. Velocities from top of the upper crust and base of the middle crust range from 4.5 km/s to 7.0 km/s with a significant gradient within the upper crust (Figure 5b). Velocity gradient within the upper crust (0 to 6 km below sediments) is strong ~0.33 km/s/km, compared to its low value within the middle crust (6 to 23 km) ~0.03 km/s/km, and intermediate value within the lower crust (23 to 28 km) ~0.08 km/s/km. According to composite lines D2 (Figure 3) and D3 (Figure 4), the upper part of the crust likely corresponds to a 20 km thick layer comprised of a large complex of superimposed wedges (these wedges are part of the Jurassic margin formed by magma-assisted extension) thickening toward the Jurassic oceanic crust and proposed to be Seaward Dipping Reflectors SDRs (Reuber et al., 2016). The lower unit is characterized by velocities significantly higher than mean continental crust defined by Christensen & Mooney (1995), ranging from 7.2 to 7.6 km/s, its average thickness is 5 km (in MAR01) and 7 km (in MAR02). Along MAR01, the lower crustal unit rapidly tapers out from 230 km model distance toward the northeast (Figure 5a). Once converted into two-way travel time, the Lower Unit in MAR02 forms an enigmatic shape below the transition domain (Figure 3) toward the Equatorial Atlantic domain. The oceanic domain is clearly identified and characterized by an approximately 5 km thick crust along both profiles. It directly overlies the mantle. However, a comparison with velocities and velocity gradients corresponding to normal oceanic crust (Figure 5d) (White et al., 1992) indicates a magmatic origin of this crust.

E-W and N-S trending composite lines

To enhance the interpretation of composite lines D2 (Figure 3) and D3 (Figure 4) which are partly coincident with the two velocity models MAR01 and MAR02, we used additional MCS line drawings oriented approximately East - West (Figure 6) and North - South (Figure 7). They cover the entire Demerara Plateau and reach the Equatorial and Central Atlantic oceanic domains (see Figure 1 for location). The composite lines D2 and D3 are is divided into: the plateau domain, the western margin with the Central Atlantic oceanic domain, and the north eastern transform and eastern rifted margins with the adjacent Equatorial Atlantic oceanic domain.

• The plateau domain

The plateau domain (Figures 3 and 4) is well constrained in composite lines. The upper part of the plateau is marked by a major erosional unconformity (Basile et al., 2013; Fanget et al., 2020) below the post Albian strata. This overlying unit is affected by major instabilities along the slopes of the plateau, especially in the north (Figure 7). These features are beyond the scope of this paper and detail descriptions are given in Loncke et al. (2009); Gaullier et al. (2010) and Pattier et al. (2015) and are synthetized in Fanget et al. (2020).

Below the Albian unconformity, an Aptian-Albian unit irregularly covers the Plateau and can be divided into two subsets. The first one is older in age and located on the western part of

the plateau (Figure 6). It is mainly located below the slope (D1 and D2) in the north. It spans the western part of the plateau (D3) in the south. This subunit can be more than two seconds thick. It is affected by numerous normal faults toward the margin, which are related to major slope instabilities above a probably inherited Jurassic relief. The second subunit appears stratigraphically younger in age and forms an extensive basin generally thinning toward the east (Figure 6, D1, D2 and D3) and the north-east where it is truncated. This subunit is affected by major compressive, apparently meridian, deformation, forming long-wavelength folds and, in some cases, related compressive faults (Figure 7, D4, D5 and D7). A detailed analysis of deformation reveals WNW – ESE fold axes, generally parallel to the northern margin of the plateau. To the north west, this subunit is affected by numerous extensive faults that cut through the Albian unconformity and portion of the overlying post-Albian strata (Figure 7), possibly due to a subordinate post-Albian extensional phase. The Albian erosional unconformity represents a significant stratigraphic gap and seals the compressive deformation.

The Aptian/Albian units were deposited above a strong amplitude seismic facies unit proposed to be Jurassic to Neocomian in age according to well FG2–1 (see Figure 1 for location), affecting the age span of the second subunit in Mercier de Lépinay (2016). This unit reaches a maximum of ~ 3 s (TWT) thickness in the northwestern part of the Plateau (Figure 6, D2 and Figure 7, D4) and progressively thins toward the east where it pinches out in the eastern part of the plateau (Figure 6) and toward the south (Figure 7). The Jurassic-Neocomian unit is affected by the compressional deformation described above. The base of the sequence is often represented by an erosional unconformity described as the post-rift Jurassic unconformity (Figures 6 and 7)

The lower part of the plateau below the post-rift unconformity is composed of fan shaped units outlined by relatively continuous and high amplitude reflectors described as Seaward (westward) Dipping Reflectors (SDRs). The whole set of SDRs lies on the deeper identified crustal Unit A. According to the velocity models, these SDR units reach a maximum thickness of ~ 7 s (TWT) or about 22 km (Figures 3 and 4) and spread over ~ 450 km from west to east (Figure 6). They can be divided into the Lower SDR, and the Upper SDR 1 and 2 that represent different shapes and regional extents. The Lower SDR unit lies on the Unit A to the east, while in the west, Unit A is covered with either Upper SDR 1 or 2. Thus, the base of SDRs is diachronous and contains faults that control the emplacement and growth of SDR bodies (Figure 6). Looking perpendicularly at the D4 and D5 sections (Figure 7) SDR units appear as basin shaped structures with no coincident depocenters. Lines D6 (Figure 6) and D7 (Figure 7) from the eastern part of the plateau reveal significant thickness of Lower SDR unit and a possible magmatic source causing symmetric SDR bodies to be emplaced. According to the velocity models (Figures 3 and 4), the western part of SDRs corresponds to the upper and middle crust of the velocity models providing a velocity range from 4.5 to 7 km/s between the Upper and Lower SDRs. Unexpectedly, the velocity structure is very stable and flat across the eastern part of the plateau (Figures 3 and 4) compared to the geometry evidenced by MCS data. It raises the question of the significance of velocity variations with concern to their related rock natures at those sites. In fact, the boundary between SDRs and Unit A is not detectable in the velocity models. In contrary to MCS lines, a distinction between SDR units and the underlying unit A is based on a change in seismic facies: from continuous and strong reflectors of SDR units to rather chaotic facies occasionally marked by strong amplitudes that may correspond to magmatic intrusions characterizing Unit A.

Below Unit A, we propose two laterally adjacent lower units (Figures 3 and 4). To the east, along velocity models MAR01 and MAR02, the existence of a deep high velocity layer

(Lower Unit 2) with values ranging from 7.2 to 7.6 km/s (Figure 5) is required to fit the arrivals observed in OBS records (Museur et al., 2021). To the west, the Lower Unit 1 corresponds to poorly reflective facies on MCS data. At this stage, there is neither proven nor obvious connection between these lower units.

• Western rifted margin and adjacent Central Atlantic oceanic domain starting with Jurassic crust

Along the western rifted margin (see Figure 1 for location), the Albian erosional unconformity and overlying layers mark the upper limit to the deformation. Below the outer western slope, the lowest levels of Post-Albian units are only deformed by few extensional faults (Figure 6).

The underlying Aptian-Albian unit reaches a thickness of ~ 3.5 s (TWT) above the present-day slope (Figure 6, D1) where it is also characterized by major west-dipping extensional faults that belong to major gravity driven slides in Cretaceous strata. On section D2 (Figure 6), the result of slope instabilities, probably controlled by an inherited topography of the Jurassic-Neocomian carbonate platform, is characterized by a bulge shape and a thick set of discontinuous deposits that progressively thin toward the basin.

The thickness of the Jurassic-Neocomian unit appears to be controlled by erosive processes involving slope failure above the present-day margin (Figure 6, D2) with a clear thinning along a paleo-slope toward the oceanic domain where it seems to fill up a graben-like structure at the transition between the interpreted oceanic crust (Figure 6, D2 and D3) and the western enigmatic margin crust (western extension of Unit A). The western edge of the carbonate platform over the volcanic series (SDRs) was already a major slope break that probably controlled the future slope evolution and hence its apparent spatial stability in time. On sections D2 and D3 (Figure 6) and with no equivalent to the north (D1), the Jurassic-Neocomian unit covers the underlying outer SDR unit toward the oceanic domain with a rather constant ~1 s (TWT) thickness.

The following lower part of the western margin is marked by the beveling of Upper SDR 1 and 2 toward the west above the possible extent of Unit A (Figure 6). However, an adjacent fan-shaped body, which also shares acoustic and geometric characteristics with SDRs, is located between the western end of the Upper SDR Unit and the interpreted oceanic domain (Figure 6, D2 and D3). This unit is called “Outer SDR” because of its location outside the plateau domain and above the more distal extent of Unit A.

Below unit A, the Lower Unit 1 is only well-imaged below the western margin on line D3 (Figure 6) where it thins toward the west. The onset of Jurassic oceanic crust is proposed on the western flank of the graben-like structure where the Moho flattens to the west. This transition is much more enigmatic on line D1 (Figure 6).

• Eastern rifted and northern transform margins of the plateau and adjacent Atlantic Equatorial oceanic domain starting with Cretaceous oceanic crust

The eastern margin is only partially, but well imaged by the eastern part of D2 section (Figure 6). The velocities are constrained by the sub-coincident MAR02 velocity model (Figure 3). It looks like a relatively narrow (less than 130 km) divergent margin composed of a few crustal tilted blocks covered with fan-shaped syn-Cretaceous rift sediments, and controlled by east-dipping normal faults. However, due to the difficulty to follow the Albian unconformity over the transitional domain, it is difficult to define which part of the Albian cretaceous strata represents a syn-rift phase. The Jurassic-Neocomian unit
appears to pinch out and onlap to the east rather than being truncated, suggesting that it was never present to the east. However, the western limit of the eastern transitional zone seems to

coincide with the more easterly extent of Jurassic SDR bodies (Figure 6) over Unit A. A coincident wide-angle velocity model reveals that within SDRs and Unit A, velocities are depth-dependent and not controlled by stratigraphy (Figure 3). To the east of the SDRs limit, Unit A forms the substratum of post Neocomian units, including post-Albian units, in a tectonically-controlled depositional system. According to MAR02 velocity model, Unit A is above the high velocity (7.2 to 7.4 km/s) Lower Unit 2, which reaches a thickness of 2–4 s (TWT) and ends toward the adjacent Cretaceous oceanic crust, well constrained by MAR02 velocity model.

The northeastern margin of the plateau corresponds to the outer corner at the junction between the transform segment and the divergent segment described above (see Figure 1 for location). It is well imaged by the northeastern part of the composite line D3 (Figure 6), and constrained by velocities of the sub-coincident MAR01 velocity model (Figures 4 and 5). It forms a wider transitional domain composed of a crustal block deformed by a system of faults with both dips directions, controlling depocenters, and filled with syn-tectonic (rift – transform) post-Neocomian – pre-Albian sediments (Figure 6, D3). The relation between extent of the transitional zone, SDRs and Unit A is very similar to that of line D2. Once again, velocities appear to be depth-dependent and not related to geometry of individual rock units, as documented by coincident MCS (Figure 4, D3). In depth, the Lower Unit 2 in profile D3 is thinner than in profile D2, i.e. around 1–2 s (TWT). To the north-east, the distal part of the transitional domain (Figure 4), prior to the unambiguous and thin oceanic crust (5 km, Figure 5), represents a domain of uncertain type. It shares some velocity characteristics with oceanic domain but its structural layout is more compatible with Unit A. Thus, this transitional domain makes it difficult for one to draw a precise Continent Ocean Boundary (COB) in this outer corner area.

The northern border of the plateau is considered to correspond to the Equatorial Atlantic transform margin (see Figure 1 for location). It is well depicted by the northeastern part of lines D4 and D5 in Figure 7. This margin corresponds to a very abrupt and steep transition between the plateau domain and the adjacent Equatorial Atlantic oceanic domain, which starts with Cretaceous crust. The Albian unconformity seals the deformation occurring in the region from the plateau down to the adjacent basin as a post-transform discontinuity. Below the plateau edge, the unconformity truncates the entire folded Aptian – Albian sequence and a part of the Jurassic-Neocomian sequence (Figure 7). Along the slope, the transform fault zone cuts through the deeper units including SDRs and Unit A. In depth, Unit A forms a prominent basement ridge. In section D5 (Figure 7), moderately deformed Lower SDR and Upper SDR 1 onlap the southern flank of the ridge. In section D4 (Figure 6) to the west, Lower SDR and Upper SDR 1 appear to be more deformed and tilted to the south thanks to a possible basement ridge uplift. However, Lower SDR and Upper SDR 1 still onlap the ridge. In accordance to this observation, we consider that the basement ridge must have existed, at least partly, prior to the first SDRs emplacement.

3.2. The Guinea Plateau

The network of seismic profiles covering the Guinea Plateau is far less dense than that on the Demerara Plateau. For comparison, a quick overview based on three seismic sections G1, G2 and G3 (Figure 8) is given in order to explore the possible continuity of deep geological structures from the Demerara TMP to the Guinea TMP.

The opening of Equatorial Atlantic has been widely debated (Moulin et al, 2010 and references therein). The authors propose a new model from the tightest reconstruction to Chron C34. For the more precise understanding of the relative positions of the Demerara Plateau,

Mercier de Lepinay (2016) proposed reconstructions obtained using the rotation poles of Moulin et al. (2010) and constrained by COB alignment and correlation between carbonate platforms and Albian slope instabilities. Despite the uncertainties in COB location and inspired by the above studies, we propose a visual hand-made morphological reconstruction that aims to connect similar geological units on either side of the Equatorial Atlantic opening trajectory (Figure 9).

Section G1 (see Figure 1 for location) is oriented WNW-ESE, presumably along the extension of section D4 from the Demerara Plateau (Figures 8 and 9). It images the crust down to 9 s (TWT). Our seismic interpretation reveals 5 major units. The upper (light-yellow) unit (Figure 8) forms a young sedimentary prism corresponding to post-Albian strata. It is separated from the older Cretaceous sequence by a major unconformity (green) that is the upper limit to a moderate deformation of the underlying layers as shown by the truncating reflectors. It looks very similar to the Albian unconformity described at the Demerara Plateau (Figure 9). The unit below the unconformity shows a less reflective facies that is slightly folded. It is characterized by a relatively homogeneous thickness of ~ 1.5 s (TWT). It is proposed to correspond to the Alptian/Albian unit of the Demerara Plateau (Figure 9). It covers a homogeneous unit (blue in Figure 8) displaying long parallel reflectors with strong amplitude, which thickens from 1 to 1.5 s (TWT) toward the SSW. It shows similar characteristics to the Jurassic-Neocomian unit of the Demerara Plateau. The underlying unit (pink in Figure 8) is composed of strong amplitude reflectors, slightly tilted to the SSW. It shares numerous characteristics with the Demerara SDR wedges (Figure 9). Its deeper unit shows a very low amplitude, contrasting with the overlying SDR sequence. It may match with a lateral equivalent of Unit A described at the Demerara Plateau (Figure 9). The last unit (orange in Figure 8) shows pale seismic facies which vertically penetrates through all the other units from a depth of ~ 7 s (TWT) to the top of post-Albian units. It corresponds to a salt diapir, rooting below the SDR units. This stratigraphic salt level occurs in several basins of the Guinea Plateau and has been dated to ~ 190 My (Jansa et al., 1980; Wade & MacLean, 1990). A juxtaposition of lines D4 and G1 (Figure 9) reveals a relative continuity and symmetry of the upper units. It also indicates the asymmetry of SDR bodies due to contradictory evolution of the underlying Unit A, forming a prominent substratum ridge along the northern border of the Demerara Plateau.

Section G2 (see Figure 1 for location) is oriented SW – NE, presumably in the basement extension of line D5 from the Demerara Plateau according to our simple reconstruction (Figure 9). It images the Guinea Plateau down to 14 s (TWT) and more or less shows the same vertical unit stacking, with a notable difference concerning the possible Jurassic-Neocomian unit and the less clear Albian unconformity. This section underlines the overall thickening of Guinea SDR bodies toward the SW, where they reach a total thickness of 4.5 s (TWT). The Moho is possibly located between depths of 11.5 and 13 s (TWT). The juxtaposition of lines D5 and G2 (Figure 9) confirms a remarkable continuity of Cretaceous and Jurassic sedimentary units and also the major asymmetry related to the basement ridge in Unit A in depth. Finally, the Moho depth is coherent between the Demerara and Guinea TMPs. The attenuated late Cretaceous deformation observed in G1 is imperceptible in the southeastern part of the Guinea Plateau and still much more severe in the northwestern Demerara Plateau (Figure 9).

Section G3 (see Figure 1 for location) is oriented WNW – ESE (Figure 8). It has been chosen to be compared to the structure of a similarly oriented line through the Demerara Plateau (Figure 9, D1). Section G3 shows a 9 s (TWT) section of the Guinea Plateau structure. The same 5 main units with specific geometry are present. It is worth noting that the SDR bodies show a similar westward thickening. The base of the SDR unit is difficult to determine on

the Guinea Plateau. However, the SDRs reach a thickness of least ~ 4 s (TWT), slightly less than the similar unit of the Demerara Plateau. Subsequently, it is hard to determine a possible lateral continuity of specific SDR units, such as the Lower SDR, that clearly pinch out against the basement ridge made in Unit A (Figure 9). The line also images the western border of the Guinea Plateau, which is marked by a distinct relief inherited from the Jurassic history of the margin that seems to control the emplacement of the interpreted Aptian/Albian units. The Albian unconformity limits the residual relief that is covered by the post-Albian strata. According to depth-converted interpretation of similarly oriented seismic line through the Guinea Plateau, Zinecker (2020) proposed that the basement unit underlying Mesozoic and Cenozoic sequences is of oceanic crustal nature. Therefore, we suggest a similar interpretation along line G3 (Figure 8). Additionally, a comparison with line D1 from the Demerara Plateau shows a similar organization of the different units (Figure 9).

4. Discussion

The aforementioned results help to specify and discuss: 1) the deep structure and nature of the Demerara TMP and their implications for the knowledge of emplacement and evolution of similar TMPs, 2) the origin and evolution of both the Guinea and Demerara TMPs.

4.1. Deep structure of conjugated TMPs

Deep structure of the Demerara Plateau

The proposed velocity models (Figures 3, 4 and 5) complement the first wide-angle study of the plateau from Greenroyd et al. (2007), which was designed to image the central western plateau. Our and their results are generally consistent in terms of velocities and unit thicknesses. However, our results provide a new insight in deep structural architecture, thanks to a large number of OBSs employed and the volume of the seismic source. In fact, the top of our new deep unit, represented by the high velocity Lower Unit, corresponds to the Moho interpreted by Greenroyd et al. (2007). At the same time, Reuber et al. (2016) pointed out the unambiguous existence of thick SDRs in the western part of the Plateau as previously suggested by Nemčok et al. (2015) and Mercier de Lépinay et al. (2016). Composite lines (Figures 3 and 4) help to correlate velocity models with reflection seismic results in order to provide additional constraints on the deeper layers including SDRs.

The deep structure of the Demerara Plateau is composed of three layers: SDRs, Unit A and Lower Unit. The upper part of the crust corresponds to a wide, generally westward-dipping (thickening) wedge of SDRs. They are proposed to be composed of varying mixtures of subaerial volcanic flows, and volcano-clastic and non-volcanic sediments (see Okay, 1995; Menzies, 2002) that can be divided into different structural types mainly based on geometric criteria (see Chauvet et al., 2020). Our SDR set is divided into Lower SDR, and Upper SDR 1 and 2, with significantly different velocity characteristics: Upper SDR between 4.5 and 6 km/s with a major vertical gradient and Lower SDR between 6 and 7 km/s (Figure 5). However, our velocity models do not show major lateral variations. At the same depth, the Lower SDR has similar velocities as the Upper SDR (5 km/s at ~8–9 km depth; 6.5 km/s at about 18 km depth). This fact negates the hypothesis that the proportion of sediment in the SDRs could explain such velocity variations (Paton et al., 2017). Subsequently, the velocity may be mainly controlled by depth and pressure (White et al., 1992) even if some other processes may be involved, such as:

weathering or hydrothermal alteration, increasing the proportion of intrusive rocks. The emplacement of the SDRs appears to be controlled by major landward-dipping extensional faults (Figure 6) according to Gibson & Love (1989); Eldholm et al. (1995); Geoffroy et al. (2015) and Chauvet et al. (2020) more than being flexure-related due to dykes or sills loading (Mutter et al., 1982; Planke & Eldholm, 1994; Paton et al., 2017).

According to composite lines D2 and D3 and the velocity models (Figures 3 and 4), the physical limit between SDRs and Unit A represents a very low acoustic impedance contrast. Unit A is proposed to be a pre-Jurassic continental crust possibly representing the Guyana Shield, injected by magmatic intrusions possibly related to volcanic events responsible for the formation of the SDRs or older events related to CAMP (Bullard et al., 1965; May, 1971; Deckart et al., 1997; Marzoli et al.; 1999; McHone, 2000; Deckart et al., 2005). Alternative interpretation can include a neoformed crust as suggested before (Gernigon et al., 2004; Reston, 2009) in a similar context, such as in the Vøring Basin where magma-affected middle crust or even magmatic crust like that of the Namibian Margin (Bauer et al., 2000) exhibit higher velocities at similar depths (7–7.5 km/s).

Lower Units 1 and 2 (Figures 3 and 4) have been determined from MCS data and wide-angle data respectively. Even if the thicknesses and depths are compatible, the lack of data in the central plateau casts doubt on their link and continuity. Wide-angle data help to constrain a velocity range from 7.2 to 7.6 km/s, comparable to a High Velocity Lower Crust (HVLC) proposed by Geoffroy et al. (2015). Such velocity ranges have been variously interpreted as 1) serpentinized mantle (O'Reilly et al., 2006), 2) volcanic underplated unit (Planert et al., 2017), and 3) pre-rifting continental crust intruded by a large amount of magmatic products (Abdelmalak et al., 2016). Clear reflected P waves from the Moho (PmP) at the base of Lower Unit observed on OBS data (Museur et al., 2021) reject the serpentinized mantle hypothesis. According to the shape, velocities and geometry, Lower Unit 1 clearly corresponds to a HVLC typical for volcanic margins (Geoffroy et al., 2015) and would, therefore, be related to Jurassic rifting. It can be either a pre-rifting continental crust intruded by a major amount of magmatic products, or an underplated magmatic material. In contrast, Lower Unit 2 has a more proximal position in respect to the Jurassic margin, and exhibits a greater thickness (3–4 s (TWT), 6–7 km according to Figure 5). It is located below the Cretaceous eastern divergent margin. Consequently, Lower Units 1 and 2 may have different origins. The Lower Unit 2 may have resulted from a distinct Cretaceous magmatic event compatible with volcanic sills proposed by Sapin et al. (2016) in the eastern transition domain and Barremian basaltic rocks found in well FG2–1 (Mercier de Lépinay et al., 2016).

Comparison with various crustal structures and geometries

The Demerara Plateau velocity structure is compared to velocity depth structures (Figure 5) of selected TMPs from Loncke et al. (2020) and LIP-type Plateau near the Agulhas TMP (Parsiegla et al., 2007). On one hand, the Demerara TMP, the Agulhas TMP, the Walvis TMP, the Faroe Bank and the Hatton-Rockall TMP (Parsiegla et al., 2007; Funck et al., 2008; White & Smith, 2009; Fromm et al., 2017) show similar trends with depth and contain comparable thicknesses that clearly differ their crust from the continental crust (Christensen & Mooney, 1995). On the other hand, the velocity depth structures of the Falklands-Malvinas TMP (Schimschal & Jokat, 2018; 2019) and the Agulhas Plateau (Parsiegla et al., 2007) are very different from those of the above-mentioned group, having clearly higher velocities and smaller thicknesses. Within the heterogeneous structure of the Falklands-Malvinas TMP (Schimschal &

Jokat, 2018; Schimschal & Jokat, 2019), only the Maurice Ewing Bank's internal block has a comparable velocity depth structure.

Comparison of the Demerara Plateau velocity structure (Figure 5) with the SE Greenland (Hopper et al., 2003) and the Namibian volcanic margins (Bauer et al., 2000) reveal strong similarities with TMPs of the first group. Moreover, the Namibian margin velocities in the upper crust and the lower crust are equivalent to those observed at the Demerara Plateau, whereas the middle crust slightly differs, possibly as a consequence of the composition and intrusive magmatism (Schön, 1996; Bauer et al., 2000).

Following, we compare (Figure 10) the key elements of the deep structure of the Demerara Plateau (Figure 10 a) including: SDRs, Unit A, Lower Unit (HVLC), with those of the Hatton-Rockall TMP (Figure 10 b), the Walvis TMP (Figure 10 c) and the Faroe Bank (Figure 10 d), all of which show a similar three-layer organization (Figure 10 b, c and d), forming comparable 25–33 km-thick plateaus even though different in width. In particular, the Walvis Ridge, characterized by the presence of an SDR complex (Elliott et al., 2009; Jegen et al., 2016; McDermott et al., 2018, Chauvet et al., 2020) a possibly thick (about 33 km), dominantly gabbroic crust (Planert et al. 2017), is interpreted as a volcanic margin associated with a hotspot trail (Gladczenko et al. 1998; Elliott et al. 2009). The Walvis Ridge shows characteristics very similar to the Demerara Plateau. They both share similar structural characteristics with well documented volcanic margins such as the Pelotas (Figure 10 f) and Namibian (Figure 10 g) margins (Bauer et al., 2000; Fernandez et al., 2010; Stica et al., 2014; Jegen et al., 2016; Planert et al., 2017) containing: 1) an SDR-dominated upper crust, 2) a middle crust called igneous crust or transitional crust possibly representing a pre-SDR crust strongly intruded by magma (Bauer et al., 2000; Fromm et al., 2017; Planert et al., 2017), and 3) a HVLC.

From another point of view, the second group composed by Falklands-Malvinas and Agulhas Plateaus (Figures 5 and 10 e) clearly differs from the Demerara Plateau. Going from west to east, the heterogeneous Falklands-Malvinas Plateau consists of the Falklands- Malvinas Plateau basin represented by a 12–20 km overthickened oceanic domain, a possible "continental" domain represented by the Maurice-Ewing Bank and the Georgia Basin oceanic domain (Schimschal & Jokat, 2019) where only the Maurice-Ewing Bank shows similar velocities to those of the Demerara Plateau (Figure 5). On the other hand, the Agulhas Plateau, which is defined as a LIP type "oceanic" plateau (Parsiegla et al., 2007), looks very similar to the Falklands-Malvinas TMP, with no evidence of either SDR complexes or HVLC even if their formation is also related to the influence of a hotspot i.e. the Karoo Hotspot (Linol et al., 2015; Hole et al., 2015).

To conclude, the first group of TMPs and volcanic margins shares the characteristic of being under hotspot influence, which explains SDR bodies and HVLC emplacement (Fowler et al., 1989; Geoffroy, 2005; White et al., 2008; Elliott et al., 2009), like the Iceland hotspot for Faroe Bank and Rockall-Hatton TMPs (Elliott et al., 2009). However, some other plateaus located in the South Atlantic Ocean, such as Falklands-Malvinas and Agulhas TMPs, seem to result from a different evolution, indicating that not all TMPs identified by Loncke et al. (2020) were formed by the same process.

Finally, our analysis leads to proposing that the structure of the Demerara Plateau corresponds to a Jurassic volcanic margin (see also Nemčok et al., 2015), which raises the question of the origin of the major volcanic products, and suggesting the possible presence of a hotspot for the Demerara Plateau, and subsequently, the Guinea region in early Jurassic. This hypothesis is confirmed by seismic data (Reuber et al.,2016) and geochemical analyses and dating of deep seafloor samples by Basile et al. (2020).

4.2. Evolution of the Demerara – Guinea conjugated TMPs

Based on our results, we present a schematic evolution of both conjugate plateaus in cross sections (Figure 11). According to kinematic plate reconstructions (Figure 2), before the opening of Central Atlantic, the Demerara-Guinea was facing to the north west the present-day Bahamas platform, Florida and, possibly, the Blake Plateau (Figure 2). Few deep penetrating seismic data are available in this area of the North America margin, but a recent compilation of gravimetric and seismic data (Dale, 2013) indicated a wide 20 km-thick domain of anomalous high-density crust located between the continental crust of Florida and the Central Atlantic oceanic crust. Density values are between 2.8 and 2.9 g/cm^3, comparable to those obtained for SDR units after conversion from wide-angle velocities (Museur et al., 2021). Therefore, the authors interpret this domain as an enigmatic LIP transitional crust. Our data also help to prove the continuity of magmatic units from Demerara to Guinea plateaus (Figures 9 and 11).

Reuber et al. (2016) were the first to propose a hotspot to explain the SDRs and the subsequent amount of volcanic products for Demerara, and proposed that this hotspot was located close to the Bahamas, to the west of the Demerara Plateau during the Jurassic period. They named it the "Bahamas hotspot". A long-lived hotspot activity generally results in a major volcanic expression forming a hotspot track according to plate motion (Morgan & Chen, 1993), which has not yet been documented for the Demerara Plateau case. During the DRADEM experiment (Basile et al., 2017), dredge samples were obtained along the steep northern transform margin of the plateau, which allowed the deeper levels to be reached. The samples reveal the geochemical signature typical for ocean island basalts (OIB). Their zircon dates to 173.4 ± 1.6 My (Basile et al., 2017). Based on these data, Basile et al., (2020) proposed a hotspot-related magmatic event, associated with the opening of the Central Atlantic and not related to the anterior CAMP volcanism (about 200 My old) at the beginning of the Demerara Plateau development.

Subsequently, Basile et al. (2020) drew a possible hotspot track, which was initially located below the Demerara Plateau at 170 My. It was possibly later responsible for the formation of the Sierra Leone Rise (Figures 2 and 5). According to this model, the Demerara Plateau may be located back above this same hotspot in the Cretaceous period. If the hypothesis concerning the possibly conjugate Bahamas-Florida margin is right, together with the Demerara – Guinea plateaus this area was corresponding to a large magmatic province 400 km long in the north-south direction and 600 km wide in the east-west direction, resulting from the Jurassic "Sierra Leone" hotspot activity.

This hotspot would have been responsible for the formation of the Demerara and Guinea volcanic margins. The presence of 190 My-old salt diapirs rooting below SDR units in the Guinea Plateau confirms (see datings in Basile et al., 2020) that the SDR body emplacement in the Guinea and Demerara region postdates the CAMP event (Figure 11) and supports the hotspot hypothesis (Reuber et al., 2016; Basile et al., 2020) with a peak event at 170 My (Basile et al., 2020). The maximum thickness of the SDR units is reached in the south-western Demerara Plateau and in the continuity with the present-day southern margin of the Guinea Plateau (Figure 11), even though they are separated by the basement ridge. We propose (Figure 11) that this prominent ridge represents a preexisting crustal relief located at the junction between the two plateaus without preventing emplacement of SDR units. Our results also illustrate the possibility of an aborted magmatic rift axis in the actual central eastern plateau (Figures 6 and 11), demonstrating the complex occurrence and polyphase tectonically-controlled emplacement of SDR bodies.

Later, during the early Cretaceous, the second phase of the history of the Guinea and Demerara Plateaus started with the development of the Equatorial Atlantic rift, possibly along pre-existing lithosphere zone of weakness and basement ridge (Figures 2 and 11). After the Jurassic evolution marked by a major post-SDR Jurassic unconformity and before the second rifting phase (Mercier de Lépinay et al., 2016), the sediment supply compensated the post-rift subsidence with the emplacement of the Jurassic-Neocomian carbonate platform along the possibly inherited relief of the volcanic margin. During Barremian/Aptian, an acceleration of subsidence is reported. A large delta characterized by gravity-driven tectonics formed west of both plateaus (Figure 11). Then, the rifting phase culminated by the progressive breakup between the Demerara and Guinea plateaus. It was delivered by a dextral shearing along a major transform fault system accompanied by deformation (Figure 2 and 11). Alongside, the eastern Demerara divergent margin is facing the Sierra Leone divergent margin. In fact, this narrow (<90 km) eastern margin of the Demerara Plateau (Figure 6) is deformed by eastward dipping normal faults bounding tilted blocks with depocenters filled by Cretaceous pre-late Albian sediments. The proximal part of this margin remarkably coincides with the easternmost extension of the SDR complex, which may have resulted from a localization of the deformation between blocks of various rheologies (Figure 11). In the transitional domain, (Figure 6) no evidence of an exhumed mantle has been found (Sapin et al., 2016). However, there is a possible underplated high velocity unit (Lower Unit 2), which may have resulted from the second rifting phase related to the Cretaceous volcanic event due to the influence of the same hotspot that was associated with the Jurassic opening (as proposed by Basile et al. (2020)).

During the Albian, both plateaus experienced major uplift and deformation. The main deformation characterized by E-W to WNW-ESE trending folds (Figure 6) was demonstrated by Gouyet (1988), Benkhelil et al. (1995), Basile et al. (2013), Mercier de Lépinay (2016). This deformation in the Guinea Plateau is far less recorded than it is in the Demerara Plateau, even though some evidence can be seen on line G1 (Figure 8). The major deformation seems to have then concentrated in the northern part of the Demerara Plateau, south of the basement ridge (Figure 7), which acted as a buttress to the transpressive tectonics preceding the final separation of the Demerara and Guinea Plateaus. In fact, folds are sometimes cut by transform related normal faults (Loncke et al., 2021). Subsequently, the transpressive tectonics is proposed to be Aptian/early Albian in age. It is related to the evolution of the stress field as a consequence of a possible rotation pole shift at Aptian-Albian limit (Rabinowitz & Labrecque, 1979; Campan, 1995; Basile et al., 2013; Reuber et al., 2016.). This led to the collision of the north of the Demerara area with the southwest of the Guinea area (Figure 11). Finally, the ultimate continental separation have led to a general collapse of the margin (Figure 11), cut by the regional and prominent upper Albian unconformity in its upper part.

5. Conclusions

This work brings new insights on the nature and the emplacement of the transform conjugate Demerara and Guinea Plateaus, thanks to wide angle seismic data and a compilation of industrial reflection seismic data. Analysis of these data reveals that Demerara and Guinea Plateaus once were a Jurassic volcanic margin. It formed the segment of the eastern Central Atlantic margin. It was composed of thick SDR units, intruded continental crust, and a high velocity lower crust. However, emplacement of the SDRs was diachronous with a possible aborted first volcanic source and tectonically controlled by a pre-existing basement ridge. This magmatic system is proposed to be controlled by the activity of the “Sierra Leone” hotspot.

This large magmatic province was reworked during the Cretaceous opening of the Equatorial Atlantic. A major transform transform fault zone developed the Northern margin of the Demerara Plateau and the Southern margin of the Guinea Plateau. The opening of the Equatorial Atlantic was predated by a compressive event recorded in the Demerara Plateau. The location of the transform margin appears to be controlled by the pre-existing basement grain whereas the Eastern rifted margin of the Demerara Plateau seems to have been located along the eastern limit of the Jurassic SDR units.

This work also discusses the characteristics of the Demerara-Guinea volcanic margin and subsequent TMPs by a comparison to similar TMPs in the Atlantic Ocean, such as the Walvis Ridge. However, not all TMPs share the same characteristics, as is exemplified by the Falklands-Malvinas and Agulhas TMPs. On the other hand, the western Jurassic margin of the Demerara TMP looks very similar to the Namibian and Pelotas volcanic margins. Of course, not all TMPs and volcanic margins have been imaged by equally robust seismic data sets. Subsequently, future studies of the structure and nature of different TMPs and volcanic margins are required to precisely explore and quantify common processes leading to their formation such as hotspots-related major thermal anomalies and superposed tectonic phases.

Acknowledgments

We thank the captain and crew of the R/Vs "*L'Atalante*" for the data acquisition during marine survey MARGATS. Further information and some data are available on the internet site of the French Oceanographic Fleet.
(https://campagnes.flotteoceanographique.fr/campagnes/16001400/fr/). T. Museur PhD Thesis was funded by the Regional Council of Bretagne and Ifremer. Access to industry MCS data was provided by TOTAL SA. Thanks to Gplates (Muller et al., 2018), Qgis, Generic Mapping Tools (Wessel and Smith, 1991), Gravity from Sandwell and Smith (2009) for figures realization.
We thank reviewers for their very helpful reviews.

References

Abdelmalak, M. M., Planke, S., Faleide, J. I., Jerram, D. A., Zastrozhnov, D., Eide, S., & Myklebust, R., 2016. The development of volcanic sequences at rifted margins: New insights from the structure and morphology of the Vøring Escarpment, mid-Norwegian Margin. Journal of Geophysical Research: Solid Earth, 121(7), 5212-5236.

Barker, P. F., 1999. Evidence for a volcanic rifted margin and oceanic crustal structure for the Falkland Plateau Basin. Journal of the Geological Society, 156 (5): 889–900. https://doi.org/10.1144/gsjgs.156.5.0889

Basile, C., Mascle, J., & Guiraud, R., 2005. Phanerozoic geological evolution of the Equatorial Atlantic domain. Journal of African Earth Sciences, 43(1-3), 275-282.

Basile, C., Maillard, A., Patriat, M., Gaullier, V., Loncke, L., Roest, W., Mercier de Lépinay, M., Pattier, F., 2013. Structure and evolution of the Demerara Plateau, offshore French Guiana: rifting, tectonic inversion and post-rift tilting at transform- divergent margins intersection. Tectonophysics 591, 16–29.

Basile, C., Girault, I., Heuret, A., Loncke, L., Poetisi, E., Graindorge, D., Deverchère, J., Klingelhoefer, F., Lebrun, J.F., Perrot, J., & Roest, W., 2017. Morphology and lithology of the continental slope north of the Demerara marginal Plateau: results from the DRADEM cruise. EGUGA, 8107

Basile, C., Girault, I., Paquette, J.L., Agranier, A., Loncke, L., Heuret, A., Poetisi, E., 2020. The Jurassic magmatism of the Demerara Plateau (offshore French Guiana) as a remnant of the Sierra Leone hotspot during the Atlantic rifting. Sci. Rep. 10 (1), 1–12.

Bauer, K., Neben, S., Schreckenberger, B., Emmermann, R., Hinz, K., Fechner, N., Gohl, K., Schulze, A., Trumbull, R., Weber, K., 2000. Deep structure of the Namibia continental margin as derived from

integrated geophysical studies. J. Geophys. Res. 105, 25829–25854. https://doi.org/10.1029/2000JB900227.

Benkhelil, J., Mascle, J., Tricart, P., 1995. The Guinea continental margin: an example of a structurally complex transform margin. Tectonophysics 248, 117–137. https://doi.org/10.1016/0040-1951(94)00246-6

Bullard, E., Everett, J.E., Smith, A.G., 1965. The fit of the continents around the Atlantic. In: Bickett, P.M.S., Bullard, E., Runcorn, S.K. (Eds.), A Symposium on Continental Drift, Philos. Trans. R. Soc. Lond., A, vol. 258, pp. 41–51.

Campan, A., 1995. Analyse Cinématique de l'Atlantique Equatorial, Implications Sur l'évolution de L'atlantique Sud et sur la Frontière de Plaque Amérique du Nord/ Amérique du Sud. PhD Thesis. Univ. "Pierre et Marie Curie", Paris VI (352 pp).

Casson, M., Jeremiah, J., Calvès, G., de Goyet, F. D. V., Reuber, K., Bidgood, M., ... & Redfern, J., 2021. Evaluating the segmented post-rift stratigraphic architecture of the Guyanas continental margin. Petroleum Geoscience, 27(3).

Chauvet, F., Sapin, F., Geoffroy, L., Ringenbach, J. C., & Ferry, J. N., 2020. Conjugate volcanic passive margins in the austral segment of the South Atlantic–Architecture and development. Earth-Science Reviews, 103461.

Christensen, N.I., Mooney, W.D., 1995. Seismic velocity structure and composition of the continental crust: a global view. J. Geophys. Res. 100 (B6), 9761–9788. https://doi. org/10.1029/95JB00259.

Dale, A. J. (2013). Crustal type, tectonic origin, and petroleum potential of the Bahamas carbonate platform (Doctoral dissertation)

Deckart, K., Bertrand, H., Liégeois, J.-P., 2005. Geochemistry and Sr, Nd, Pb isotopic composition of the Central Atlantic Magmatic Province (CAMP) in Guyana and Guinea. Lithos 82, 282–314. https://doi.org/10.1016/j.lithos.2004.09.023.

Deckart, K., Féraud, G., Bertrand, H., 1997. Age of Jurassic continental tholeiites of French Guyana, Surinam and Guinea: implications for the initial opening of the Central Atlantic Ocean. Earth Planet. Sci. Lett. 150, 205–220.

Eldholm, O., Skogseid, J., Planke, S., Gladczenko, T.P., 1995. Volcanic margin concepts. Springer 463. https://doi.org/10.1007/978-94-011-0043-4_1.

Elliott, G., Berndt, C., Parson, L., 2009. The SW African volcanic rifted margin and the initiation of the Walvis Ridge, South Atlantic. Marine Geophysical Research. 30. 207-214. 10.1007/s11001-009-9077-x.

Erbacher, J., Mosher, D.C., Malone, M.J., Sexton, P., Wilson, P.A., 2004. Proceedings of the Ocean Drilling Program, Initial Reports. Vol. 207. Demerera Rise: equatorial Cretaceous and Paleogene paleoceanographic transect, Western Australia. Covering Leg 207 of the cruises of the Drilling Vessel" Joides Resolution", Bridgetown, Barbados, to Rio de Janeiro, Brazil, Sites 1257-1261, 11 January-6 March 2003. Texas A & M University Ocean Drilling Program.

Fanget, A.N., Loncke, L., Pattier, F., Marsset, T., Roest, W., Tallobre, C., Durrieu de Madron, X., Hernández-Molina, F., 2020. A synthesis of the sedimentary evolution of the Demerara Plateau (Central Atlantic Ocean) from the late Albian to the Holocene. Marine and Petroleum Geology. 104195. 10.1016/j.marpetgeo.2019.104195.

Fernandez, M., Afonso, J., Ranalli, G., 2010. The deep lithospheric structure of the Namibian volcanic margin. Tectonophysics 481. https://doi.org/10.1016/j. tecto.2009.02.036.

Fowler, S.R., White, R.S., Spence, G.D., Westbrook, G.K., 1989. The Hatton Bank continental margin—II. Deep structure from two-ship expanding spread seismic profiles. Geophysical Journal International 96 (2), 295–309.

Fromm, T., Jokat, W., Ryberg, T., Behrmann, J., Haberland, C., Weber, M., 2017. The onset of Walvis Ridge: Plume influence at the continental margin. Tectonophysics 716, 90–107. https://doi.org/10.1016/j.tecto.2017.03.011.

Funck, T., Morten Sparre, A., Neish, J., Dahl-Jensen, T., 2008. A refraction seismic transect from the Faroe Islands to the Hatton-Rockall Basin. J. Geophys. Res. 113 https://doi.org/10.1029/2008JB005675.

Gaullier, V., Loncke, L., Droz, L., Basile, C., Maillard, A., Patriat, M., ... & Carol, F., 2010. Slope instability on the French Guiana transform margin from swath-bathymetry and 3.5 kHz echograms. In *Submarine Mass Movements and Their Consequences* (pp. 569-579). Springer, Dordrecht.

Geoffroy, L., 2005. Volcanic passive margins. Comptes Rendus Geoscience, 337(16), 1395-1408.

Geoffroy, L., Burov, E.B., Werner, P., 2015. Volcanic passive margins: another way to break up continents. Sci. Rep. 5 (1), 1–12.

Gernigon, L., Ringenbach, J.C., Planke, S., Le Gall, B., 2004. Deep structures and breakup along volcanic rifted margins: insights from integrated studies along the outer Vøring Basin (Norway). Marine and Petroleum Geology 21(3), 363–372.

Gibson, I., Love, D., 1989. A listric Fault Model for the Formaztion of the Dipping Reflectors Penetrated during the Drilling of the Hole 642E, ODP 104. Scientific Results 104, 979–983. https://doi.org/10.2973/odp.proc.sr.104.195.1989.

Gladczenko, T. P., Skogseid, J., & Eldhom, O., 1998. Namibia volcanic margin. Marine geophysical researches, 20(4), 313-341.

Gouyet, S., 1988. Évolution tectono-sédimentaire des marges guyanaise et nord-brésilienne au cours de l'évolution de l'Atlantique Sud. PhD Thesis. Univ. " Pau et des pays de l'Adour " (374 pp).

Graindorge, D., Klingelhoefer, F., 2016. MARGATS cruise, RV L'Atalante, https://doi.org/10.17600/16001400

Greenroyd, C. J., Peirce, C., Rodger, M., Watts, A. B., & Hobbs, R. W., 2007. Crustal structure of the French Guiana margin, west equatorial Atlantic. Geophysical Journal International, 169(3), 964-987.

Greenroyd, C. J., Peirce, C., Rodger, M., Watts, A.B., Hobbs, R.W., 2008. Demerara Plateau- the structure and evolution of a transform passive margin. Geophysical Journal International 172, 549–564. https://doi.org/10.1111/j.1365-246X.2007.03662.x

Griffith, C.P., 2017. Evidence for a Jurassic Source Rock in the Guiana-Suriname Basin. AAPG Datapages/Search and Discovery Article #90291, AAPG Annual Convention and Exhibition, Houston, Texas, April 2-5, 2017.

Hole, M., Ellam, R., Macdonald, D., Kelley, S., 2015. Gondwana break-up related magmatism in the Falkland Islands. J. Geol. Soc. https://doi.org/10.1144/ jgs2015-027.

Hopper, J.R., Dahl-Jensen, T., Holbrook, W.S., Larsen, H.C., Lizarralde, D., Korenaga, J., Kelemen, P.B., 2003. Structure of the SE Greenland margin from seismic reflection and refraction data: Implications for nascent spreading center subsidence and asymmetric crustal accretion during North Atlantic opening. Journal of Geophysical Research: Solid Earth 108 (B5).

Jansa, L. F., Bujak, J. P., & Williams, G. L., 1980. Upper Triassic salt deposits of the western North Atlantic. Canadian Journal of Earth Sciences, 17(5), 547-559.

Jegen, M., Avdeeva, A., Berndt, C., Franz, G., Heincke, B., Ho Ï z, S., Kopp, H., 2016. 3-D magnetotelluric image of offshore magmatism at the Walvis Ridge and rift basin. Tectonophysics 683, 98–108.

Klingelhoefer, F., Edwards, R. A., Hobbs, R. W., and England, R. W., 2005. Crustal structure of the NE Rockall Trough from wide-angle seismic data modeling, J. Geophys. Res., 110, B11105, doi:10.1029/2005JB003763.

Klitgord, K. D., and Schouten, H., 1986. Plate kinematics of the central Atlantic. *in* (Vogt, P. R., and Tucholke, B. E. Eds.), *The Geology of North America, Volume M*, The Western North Atlantic Region, Geological Society of America, 351-378.

Labails, C., Olivet, J.-L., Aslanian, D., Roest, W.R., 2010. An alternative early opening scenario for the Central Atlantic Ocean. Earth and Planetary Science Letters 297, 355–368. https://doi.org/10.1016/j.epsl.2010.06.024

Leitchenkov, G., Guseva, J., Gandyukhin, V., Grikurov, G., Kristoffersen, Y., Sand, M., Aleshkova, N., 2008. Crustal structure and tectonic provinces of the Riiser-Larsen Sea area (East Antarctica): results of geophysical studies. Marine Geophysical Research, 29(2), 135- 158.

Linol, B., deWit, M.J., Guillocheau, F., Robin, C., Dauteuil, O., deWit, M.J., Guillocheau, F., deWit, M.J.C., 2015. Multiphase Phanerozoic subsidence and uplift history recorded in the Congo Basin: a complex

successor basin. In: Geology and Resource Potential of the Congo Basin. Springer-Verlag, Berlin Heidelberg, pp. 213–227.

Loncke, L., Droz, L., Gaullier, V., Basile, C., Patriat, M., & Roest, W., 2009. Slope instabilities from echo-character mapping along the French Guiana transform margin and Demerara abyssal plain. Marine and Petroleum Geology, 26(5), 711-723.

Loncke, L., Droz, L., Gaullier, V., Basile, C., Patriat, M., & Roest, W., 2009. Slope instabilities from echo-character mapping along the French Guiana transform margin and Demerara abyssal plain. Marine and Petroleum Geology, 26(5), 711-723.

Loncke, L., Maillard, A., Basile, C., Roest, W. R., Bayon, G., Gaullier, V., Marsset, T., 2016. Structure of the Demerara passive-transform margin and associated sedimentary processes. Initial results from the IGUANES cruise. Geological Society, London, Special Publications, 431(1), 179-197.

Loncke, L., Roest, W.R., Klingelhoefer, F., Basile, C., Graindorge, D., Heuret, A., Marcaillou, B., Museur, T., Fanget, A.S., Mercier de Lépinay, M., 2020. Transform Marginal Plateaus. Earth-Science Reviews 203, 102940. https://doi.org/10.1016/j.earscirev.2019.102940

Loncke, L., de Lépinay, M. M., Basile, C., Maillard, A., Roest, W. R., De Clarens, P., ... & Sapin, F. (2021). Compared structure and evolution of the conjugate Demerara and Guinea transform marginal plateaus. Tectonophysics, 229112.

Marinho, M., Mascle, J., & Wannesson, J. (1988). Structural framework of the southern Guinean margin (central Atlantic). Journal of African Earth Sciences (and the Middle East), 7(2), 401-408.

Marzoli, A., Renne, P. R., Piccirillo, E. M., Ernesto, M., Bellieni, G., and De Min, A., 1999. Extensive 200-million- year-old continental flood basalts of the Central Atlantic Magmatic Province, Science, 284(5414), 616- 618.

Marzoli, A., Renne, P. R., Piccirillo, E. M., Ernesto, M., Bellieni, G., and De Min, A., 1999. Extensive 200-million-year-old continental flood basalts of the Central Atlantic Magmatic Province, *Science*, *284*(5414), 616-618.

Mascle, J., Marinho, M. and Wannesson, J., 1986. The structure of the Guinean continental margin: implications for the connection between the central and the South Atlantic oceans. *Geol. Rundschau*., *75*(1), 57-70.

May, P.R., 1971. Patterns of Triassic diabase dikes around the North Atlantic in the context of predrift position of the continents. Geol. Soc. Am. Bull. 82, 1285–1292.

McDermott, C., Lonergan, L., Collier, J. S., McDermott, K. G., & Bellingham, P., 2018. Characterization of Seaward-Dipping Reflectors Along the South American Atlantic Margin and Implications for Continental Breakup. Tectonics, 37(9), 3303-3327.

McHone, G.J., 2000. Non-plume magmatism and rifting during the opening of the Central Atlantic Ocean. Tectonophysics 316, 287–296.

McMaster, R. L., Lachance T. P., and Ashraf, A., 1970. Continental shelf geomorphic features off Portuguese Guinea, Guinea, and Sierra Leone (West Africa), *Marine Geology, 9*, 203-213.

Menzies, M.A. (Ed.), 2002. Volcanic rifted margins, vol. 362. Geological Society of America.

Mercier de Lépinay, M., 2016. Inventaire mondial des marges transformantes et évolution tectono-sédimentaire des plateaux de Demerara et de Guinée. PhD Thesis. Univ. Perpignan.

Mercier de Lépinay, M., Loncke, L., Basile, C., Roest, W. R., Patriat, M., Maillard, A., & De Clarens, P., 2016. Transform continental margins—Part 2: A worldwide review. Tectonophysics, 693, 96–115. https://doi.org/10.1016/j.tecto.2016.05.038

Morgan, J. P., and Chen, Y. J., 1993. The genesis of oceanic crust: Magma injection, hydrothermal circulation, and crustal flow, J. Geophys. Res., 98(B4), 6283– 6297, doi:10.1029/92JB02650.

Mosher, D.C., Erbacher, J., Malone, M.J. (Eds.), 2007. Proceedings of the Ocean Drilling Program, 207 Scientific Results, Proceedings of the Ocean Drilling Program. Ocean Drilling Program. https://doi.org/10.2973/odp.proc.sr.207.2007

Moulin, M., Aslanian, D., Unternehr, P., 2010. A new starting point for the South and Equatorial Atlantic Ocean. Earth-Science Reviews 98, 1–37. https://doi.org/10.1016/j.earscirev.2009.08.001

Müller, R. D., Cannon, J., Qin, X., Watson, R. J., Gurnis, M., Williams, S., et al. 2018. GPlates: Building a virtual Earth through deep time. Geochemistry, Geophysics, Geosystems, 19. doi:10.1029/2018GC007584.

Museur, T., Graindorge, D., Klingelhoefer, F., Roest, W. R., Basile, C., Loncke, L., & Sapin, F., 2021. Deep structure of the Demerara Plateau: From a volcanic margin to a Transform Marginal Plateau. Tectonophysics, 803, 228645.

Museur, T., 2020. Caractérisation de la structure profonde du Plateau de Démérara, au large de la Guyane et du Suriname. PhD Thesis. Univ. Bretagne Occidentale (247 pp).

Mutter, J.C., Talwani, M., Stoffa, P.L., 1982. Origin of seaward-dipping reflectors in oceanic crust off the Norwegian margin by "subaerial sea-floor spreading". Geology 10(7), 353–357.

Nemčok, M., Rybár, S., Odegard, M., Dickson, W., Pelech, O., Ledvényiová, L., Matejová, M., Molčan, M., Hermeston, S., Jones, D., Cuervo, E., Cheng, R. and Forero, G., 2015. Development history of the southern terminus of the Central Atlantic; Guyana-Suriname case study. In: Nemčok, M., Rybár, S., Sinha, S. T., Hermeston, S. A. and Ledvényiová, L., (Eds), 2015. Transform margins: development, controls and petroleum systems. Geological Society of London Special Publication No 431, http://doi.org/10.1144/SP431.10.

Okay, Nilgun, 1995. Thermal Development and Rejuvenation of the Marginal Plateaus along the Transtensional Volcanic Margins of the Norwegian-Greenland Sea.

Olyphant, J.R., Johnson, R.A., Hughes, A.N., 2017. Evolution of the Southern Guinea Plateau: implications on Guinea-Demerara Plateau formation using insights from seismic, subsidence, and gravity data. Tectonophysics 717, 358–371.

O'Reilly, B., Hauser, F., Ravaut, C., Shannon, P., Readman, P., 2006. Crustal thinning, mantle exhumation and serpentinization in the Porcupine Basin, offshore Ireland: evidence from wide-angle seismic data. J. Geol. Soc. 163, 775–787. https://doi.org/ 10.1144/0016-76492005-079.

Parsiegla, N., Gohl, K., Uenzelmann-Neben, G., 2007. Deep crustal structure of the sheared South African continental margin: first results of the Agulhas-Karoo Geoscience Transect. S. Afr. J. Geol. 110 (2–3), 393–406.

Paton, D., Pindell, J., McDermott, K., Bellingham, P., Horn, B., 2017. Evolution of seaward-dipping reflectors at the onset of oceanic crust formation at volcanic passive margins: insights from the South Atlantic. Geology 45. https://doi.org/10.1130/ G38706.1.

Pattier, F., Loncke, L., Gaullier, V., Basile, C., Maillard, A., Imbert, P. and Loubrieu, B., 2013. Mass-transport deposits and fluid venting in a transform margin setting, the eastern Demerara Plateau (French Guiana). Marine and Petroleum Geology, 46, 287-303.

Pattier, F., Loncke, L., Imbert, P., Gaullier, V., Basile, C., Maillard, A., Roest, W.R., Patriat, M., Vendeville, B.C., Marsset, T., 2015. Origin of an enigmatic regional Mio-Pliocene unconformity on the Demerara Plateau. Marine Geology 365, 21–35.

Pindell, J.L., Kennan, L., 2009. Tectonic evolution of the Gulf of Mexico, Caribbean and northern South America in the mantle reference frame: an update. Geological Society, London, Special Publications 328, 1–55.

Planert, L., Behrmann, J., Jokat, W., Fromm, T., Ryberg, T., Weber, M., Haberland, C., 2017. The wide-angle seismic image of a complex rifted margin, offshore North Namibia: implications for the tectonics of continental breakup. Tectonophysics 716, 130–148.

Planke, S., Eldholm, O., 1994. Seismic response and construction of seaward dipping wedges of flood basalts: Vøring volcanic margin. Journal of Geophysical Research: Solid Earth 99(B5), 9263–9278.

Rabinowitz, P.D. & La Brecque, J., 1979. The Mesozoic South Atlantic Ocean and evolution of its continental margins, Journal of Geophysical Research 84(B11), 5973–6001.

Reston, T.J., 2009. The structure, evolution and symetry of the magma-poor rifted margins of the North and Central Atlantic: A synthesis. Tectonophysics 468 (1–4), 6–27.

Reuber K., Pindell J., Horn B., 2016. Demerara Rise, offshore Suriname: Magma-rich segment of the Central Atlantic Ocean, and conjugate to the Bahamas hotspot. Interpretation, 4(2), T141-T155. doi: 10.1190/INT-2014-0246.1

Sandwell, D. T., & Smith, W. H., 2009. Global marine gravity from retracked Geosat and ERS-1 altimetry: Ridge segmentation versus spreading rate. Journal of Geophysical Research: Solid Earth, 114(B1).Sapin, F., Davaux, M., Dall'Asta, M., Lahmi, M., Baudot, G., Ringenbach, J.-C., 2016. Post-rift subsidence of the French Guiana hyper-oblique margin: from rift-inherited subsidence to Amazon deposition effect. Geological Society, London, Special Publications 431, 125–144.

Sapin, F., Davaux, M., Dall'Asta, M., Lahmi, M., Baudot, G., Ringenbach, J.C., 2016. Post- rift subsidence of the French Guiana hyper-oblique margin: from rift-inherited subsidence to Amazon deposition effect. Geol. Soc. Lond., Spec. Publ. 431 (1), 125–144.

Sayers, B., Cooke, R., 2018. The MSGBC Basin, Geoexpro, Vol. 15, No. 5.

Schimschal, C.M., Jokat, W., 2018. The crustal structure of the continental margin east of the Falkland Islands. Tectonophysics 724-725, 234–253. https://doi.org/10.1016/j. tecto.2017.11.034.

Schimschal, C.M., Jokat, W., 2019. The crustal structure of the Maurice Ewing Bank. Tectonophysics 769, 228190.

Schön, J.H., 1996. Physical Properties of Rocks: Fundamentals and Principles of Petrophysics, vol. 18. Handbook of Geophysical Exploration. Seismic Exploration.

Sheridan, R. E., Houtz, R. E., Drake, C. L., and Ewing, M., 1969. Structure of continental margin off Sierra Leone, West Africa; *Journal of Geophysical Research*, *74*(10), 2512-2530.

Stica, J. M., Zalán, P. V., & Ferrari, A. L., 2014. The evolution of rifting on the volcanic margin of the Pelotas Basin and the contextualization of the Paraná–Etendeka LIP in the separation of Gondwana in the South Atlantic. Marine and Petroleum Geology, 50, 1-21.

Tallobre, C., Loncke, L., Bassetti, M. A., Giresse, P., Bayon, G., Buscail, R., Sotin, C., 2016. Description of a contourite depositional system on the Demerara Plateau: Results from geophysical data and sediment cores. Marine Geology, 378, 56-73.

Villeneuve, M., & Cornée, J. J., 1994. Structure, evolution and palaeogeography of the West African craton and bordering belts during the Neoproterozoic. Precambrian Research, 69(1-4), 307-326.

Vogt, U., Makris, J., O'Reilly, B.M., Hauser, F., Readman, P.W., Jacob, A.B., Shannon, P. M., 1998. The Hatton Basin and continental margin: crustal structure from wide- angle seismic and gravity data. J. Geophys. Res. Solid Earth 103 (B6), 12545–12566.

Wade, J.A, MacLean, B.C., 1990. The Geology of the southeastern margin of Canada, M.J Keen, C.A Williams (Eds.), Geology of Canada, Geology of the Continental Margin of Eastern Canada, Geological Survey of Canada (1990), pp. 167-238

Welford, J.K., Shannon, P.M., O'Reilly, B.M., Hall, J., 2012. Comparison of lithosphere structure across the Orphan Basin–Flemish Cap and Irish Atlantic conjugate continental margins from constrained 3D gravity inversions. J. Geol. Soc. 169 (4), 405–420.

Wessel, P., & Smith, W. H., 1991. Free software helps map and display data. Eos, Transactions American Geophysical Union, 72(41), 441-446.

White, R.S., Smith, L.K., 2009. Crustal structure of the Hatton and the conjugate East Greenland rifted volcanic continental margins, NE Atlantic. J. Geophys. Res. Solid Earth 114 (B2).

White, R.S., McKenzie, D., O'Nions, R.K., 1992. Oceanic crustal thickness from seismic measurements and rare earth element inversions. J. Geophys. Res. 97 (B13), 19683–19715. https://doi.org/10.1029/92JB01749.

White, R.S., Smith, L.K., Roberts, A.W., Christie, P.A.F., Kusznir, N.J., 2008. Lower- crustal intrusion on the North Atlantic continental margin. Nature 452 (7186), 460.

Zelt, C. A., & Smith, R. B., 1992. Seismic traveltime inversion for 2-D crustal velocity structure. Geophysical journal international, 108(1), 16-34.

Zinecker, M. P. (2020). Structural and Stratigraphic evolution of three Mesozoic, rifted passive margins: Guinea Plateau, Demerara Rise and Southern Gulf of Mexico. PhD Thesis. Univ. of Houston (302 pp).

Figure Captions

Figure 1*: Bathymetric (depths in meters) maps of the Demerara A) and Guinea B) conjugated Transform Marginal Plateaus. Location of the presented synthetic line drawings from the Guinea TMP: G1 to G3, and from the Demerara TMP: D1 to D7. Location of velocity models from the MARGATS experiment MAR01 and MAR02 in red; GB: Guyana Basin; SLNEA: Southern Limit of the Northern Equatorial Atlantic, GFZ: Guinea Fracture Zone.*

Figure 2*: Location of Demerara and Guinea TMPs at the present (0 My); Maps represent the free air gravity anomaly (Sandwell and Smith, 2009); Central and Equatorial Atlantic are labeled respectively in blue and green; FZ: Fracture Zone, GFZ: Guinea FZ, CFZ: Cap Vert FZ, MFZ: Marathon FZ, VFZ: Vema FZ, DFZ: Doldrums FZ, SFZ: Strakhov FZ, StPFZ: Saint Paul FZ, RFZ: Romanche FZ, 15°20'FZ, SLR: Sierra Leone Rise; Kinematic reconstructions at 104, 124, 154 and 170 My, performed with GPlates using rotation poles from earlier studies (Campan, 1995; Moulin et al., 2010); positions of Sierra Leone hotspot is from Basile et al. (2020); GB: Guyana Basin.*

Figure 3*: Composite line D2 through the Demerara Plateau (see figure 1 for location), composed of MCS data in the west and combined wide-angle (MAR02) and MCS data in the east; detailed comparison of Vz profile within different domains with Vz "standard" of continental and oceanic crusts (Christensen and Mooney, 1995; White et al., 1992), modified after Museur et al., 2021.*

Figure 4*: Composite line D3 through the Demerara Plateau (see figure 1 for location) composed of MCS data in the west and combined wide-angle (MAR01) and MCS data to the north-east; detailed comparison of Vz profile within different domains with Vz "standard" of continental and oceanic crusts (Christensen and Mooney, 1995; White et al., 1992), modified after Museur et al. (2021).*

Figure 5*: a) velocity model MAR01 see Museur et al. (2021) for details; b), c) and d) Vz comparison between different domains of the Demerara Plateau and continental and oceanic crusts (Christensen and Mooney , 1995; White et al., 1992); e), f) and g) Vz comparisons with other TMPs similar to the Demerara Plateau: the Walvis Ridge (Planert et al., 2017), the Agulhas TMP (Parsiegla et al., 2007), the Faroe Bank (Funck et al., 2008), the Hatton Bank (White and Smith, 2009), the Rockall Bank (Vogt et al., 1998); h) Vz synthesis of TMPs; i), j), k) and l) Vz comparisons with other TMPs different from the Demerara Plateau: the Falklands-Malvinas Bank (Schimschal and Jokat, 2018; Schimschal and Jokat, 2019), the Central Agulhas Plateau (Parsiegla et al., 2007); m) and n) Vz comparisons with volcanic margins: the SE Greenland margin (Hopper et al., 2003) and the Namibian margin (Bauer et al., 2000).*

Figure 6*: Line drawings and interpretations of composite Demerara Plateau lines D1, D2, D3 and D6 (see figure 1 for location). D2 and D3 are obtained from interpretation of sub-coincident MCS and wide-angle data.*

Figure 7*: Line drawings and interpretations of Demerara Plateau composite lines D4, D5 and D7 (see figure 1 for location).*

Figure 8*: Line drawings and interpretations of Guinea Plateau lines G1, G2 and G3 (see figure 1 for location).*

Figure 9*: Comparison of WNW-ENE sections of Demerara (D1) and Guinea (G3) TMPs shown in the same scale across the Jurassic volcanic margin. Inset shows our hand-made morphological reconstruction based on Moulin et al. (2010) and Mercier de Lépinay (2016) works, made for a time period of 125 My. Lowermost two profiles represent our attempt to put line drawings of sections D4 and D5 from the Demerara TMP and G1 and G2 for the Guinea TMP face to face at the same scale.*

Figure 10*: Comparison between crustal structures of : a) the Demerara Plateau (Modified from Reuber et al., 2016 and Museur et al., 2021); b) the Hatton Bank (Fowler et al., 1989); c) the Walvis Ridge (From Planert et al., 2017; Jegen et al., 2016); d) the Faroe Bank (White et al., 2008); e) the Falklands-Malvinas TMP (Schimschal and Jokat, 2018, 2019); f) the Pelotas Volcanic Margin (Stica et al., 2014); g) the Namibian Volcanic Margin (Bauer et al., 2000; Fernandez et al., 2010); After Museur et al., 2021.*

Figure 11*: Left: schematic evolution of both conjugated plateaus from a north-south point of view (R1); Right: schematic evolution of the Demerara Plateau from a west-east point of view (R2); Lower-left hand-made morphological reconstruction based on Moulin et al. (2010) and Mercier de Lépinay (2016), probably around 125 My (see also Figure 2).*

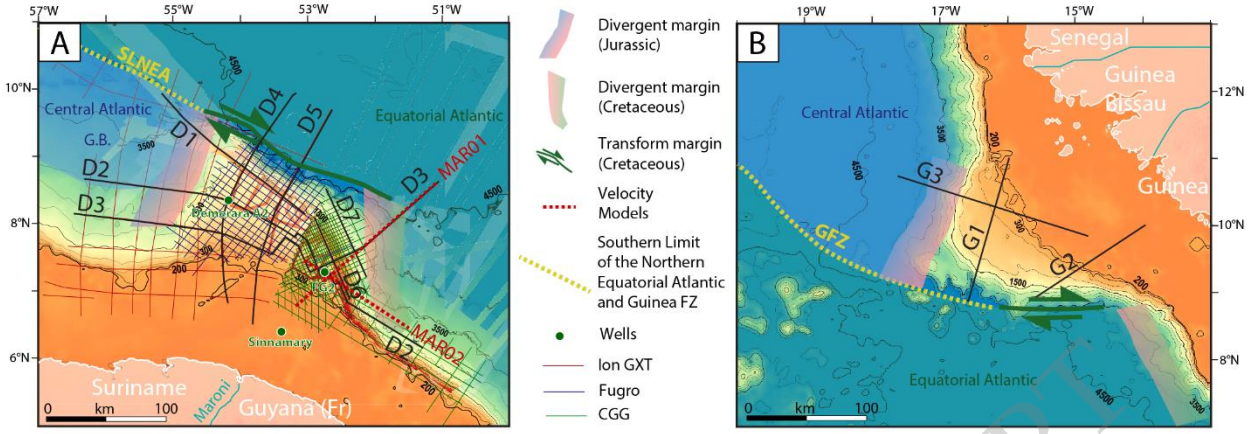

Figure 1

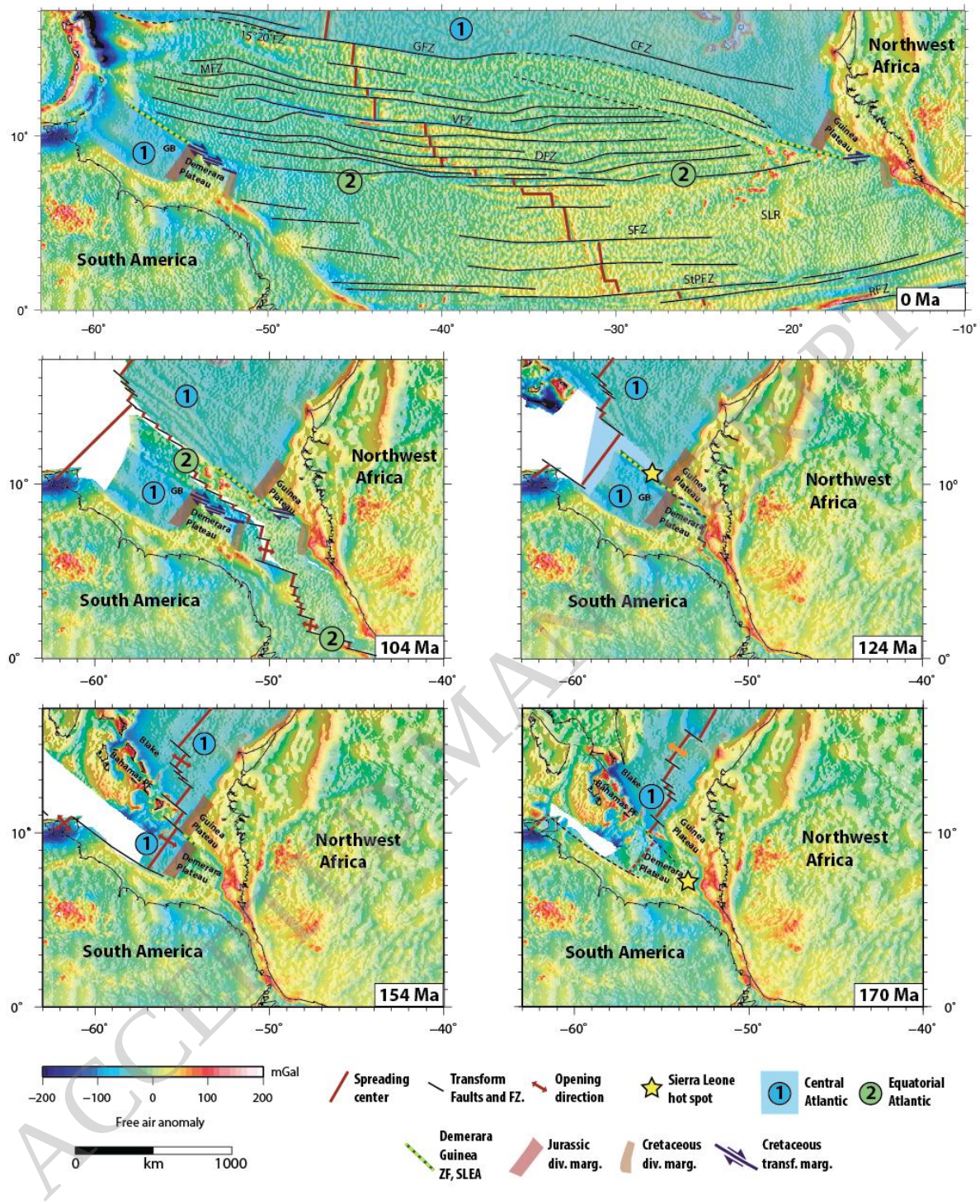

Figure 2

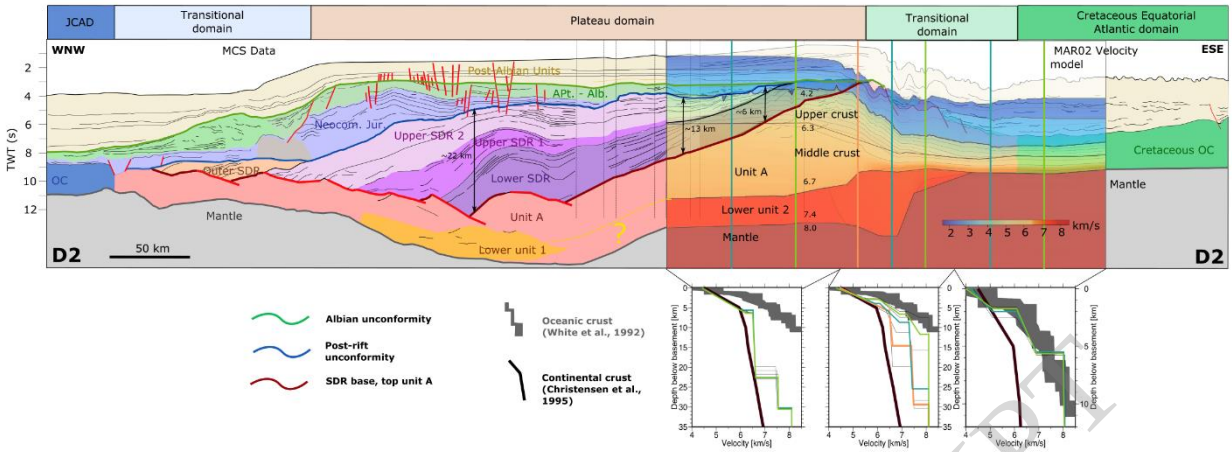

Figure 3

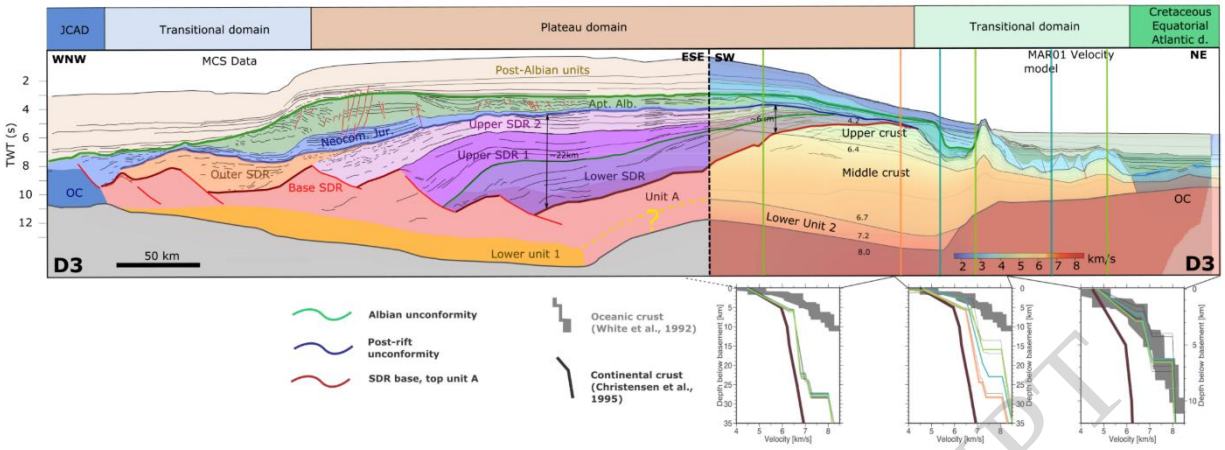

Figure 4

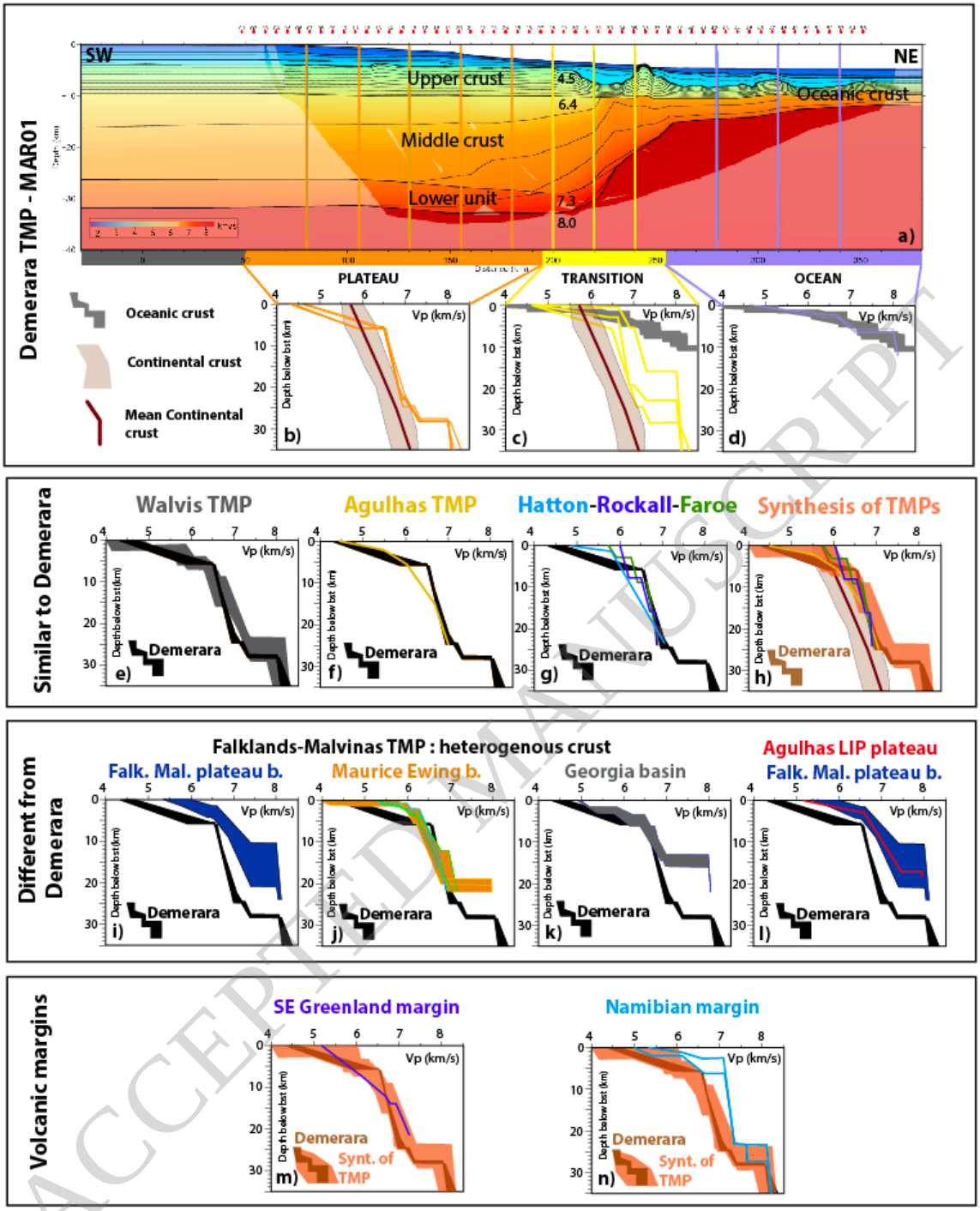

Figure 5

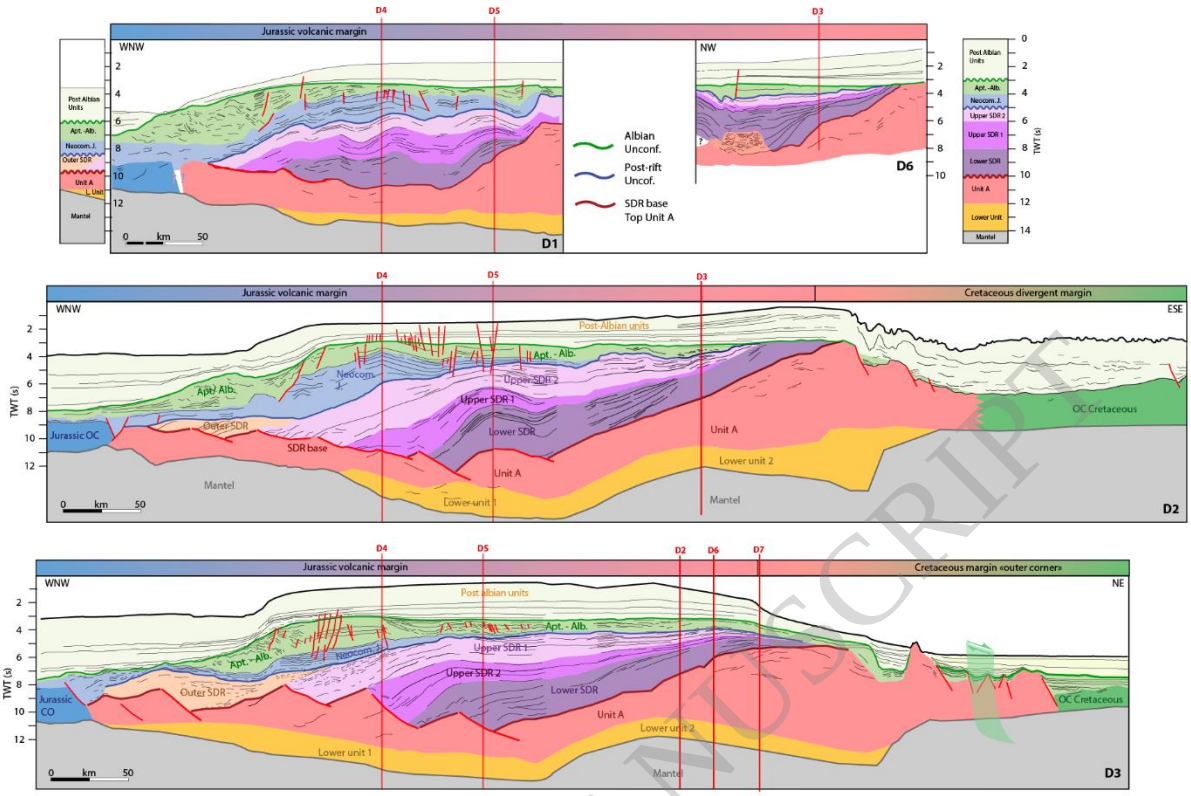

Figure 6

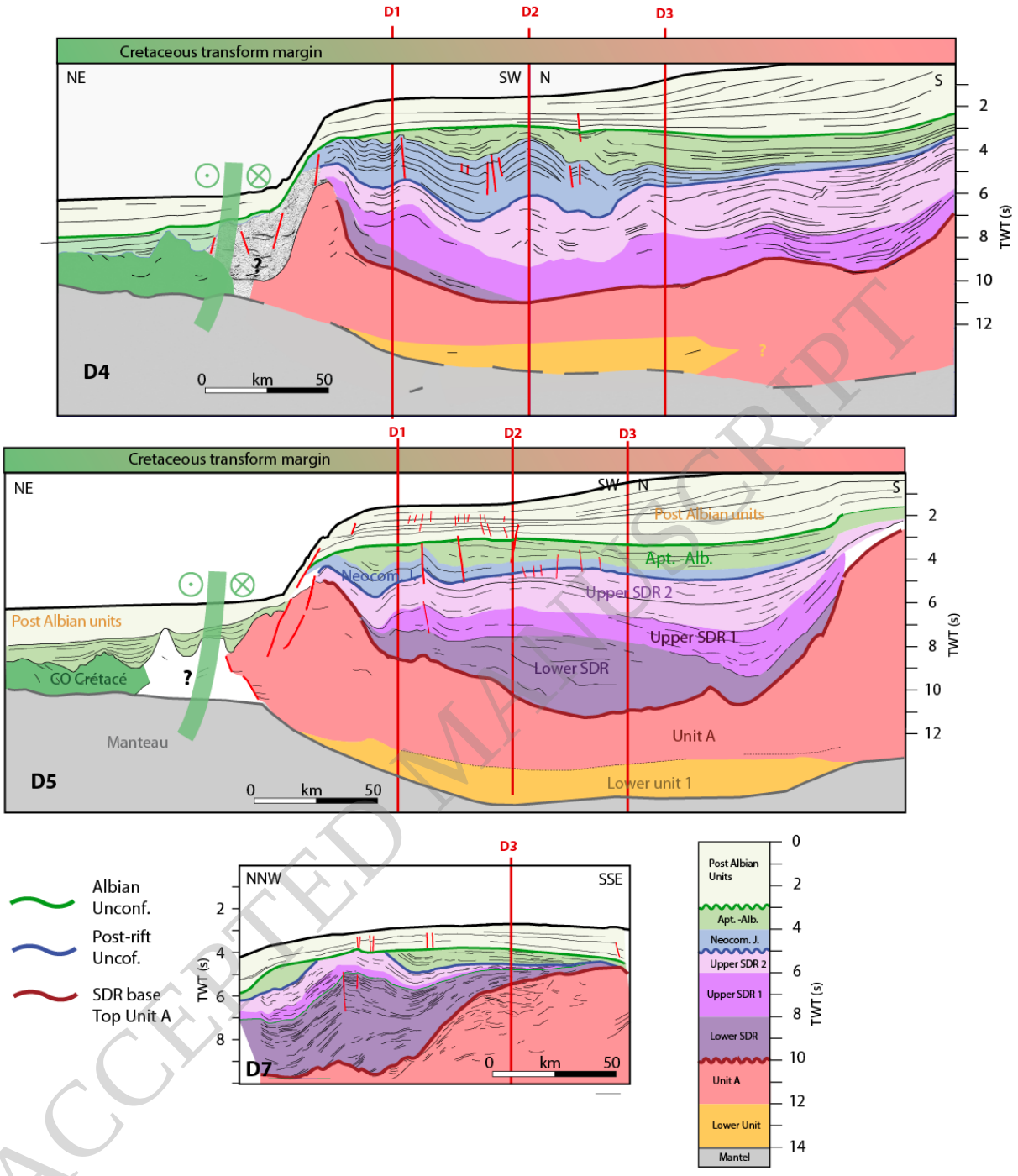

Figure 7

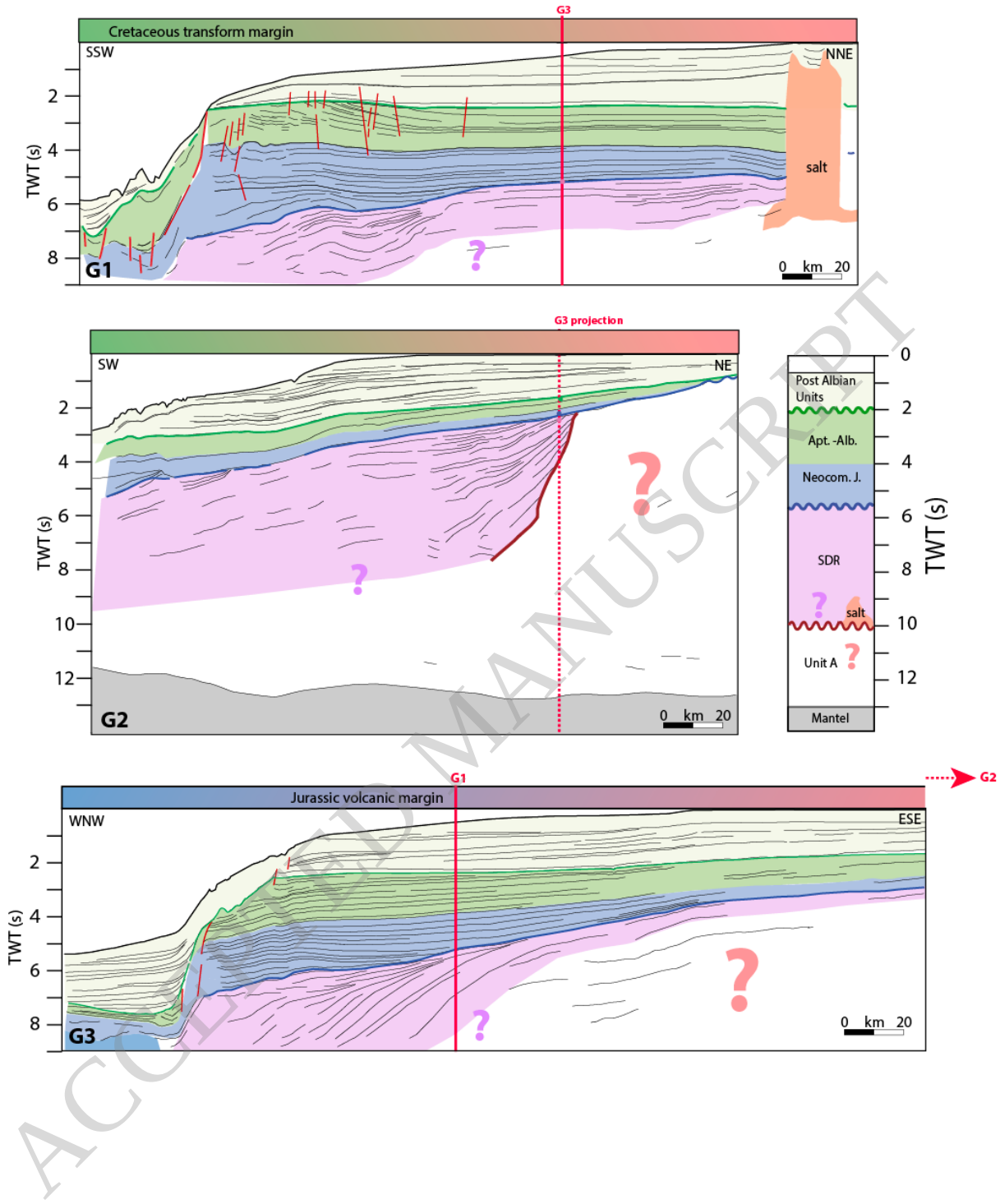

Figure 8

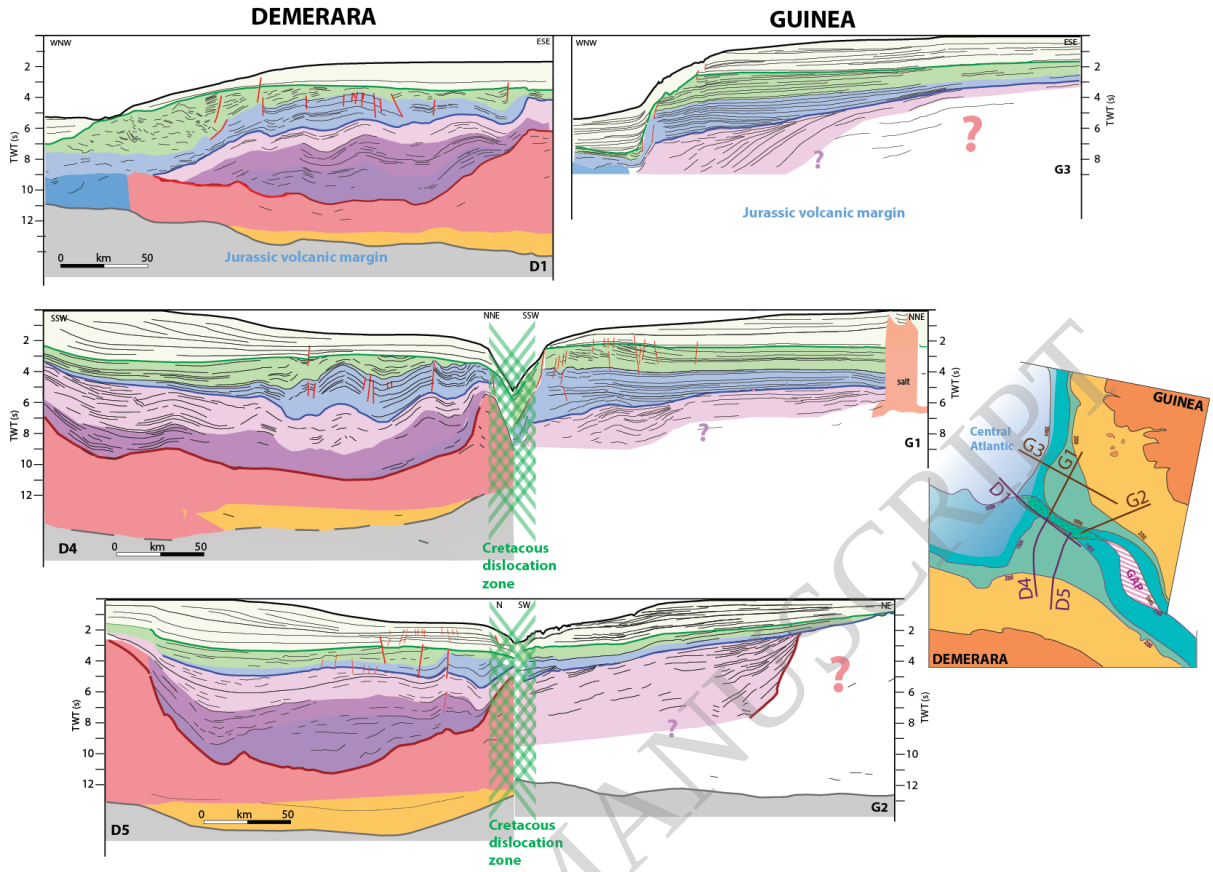

Figure 9

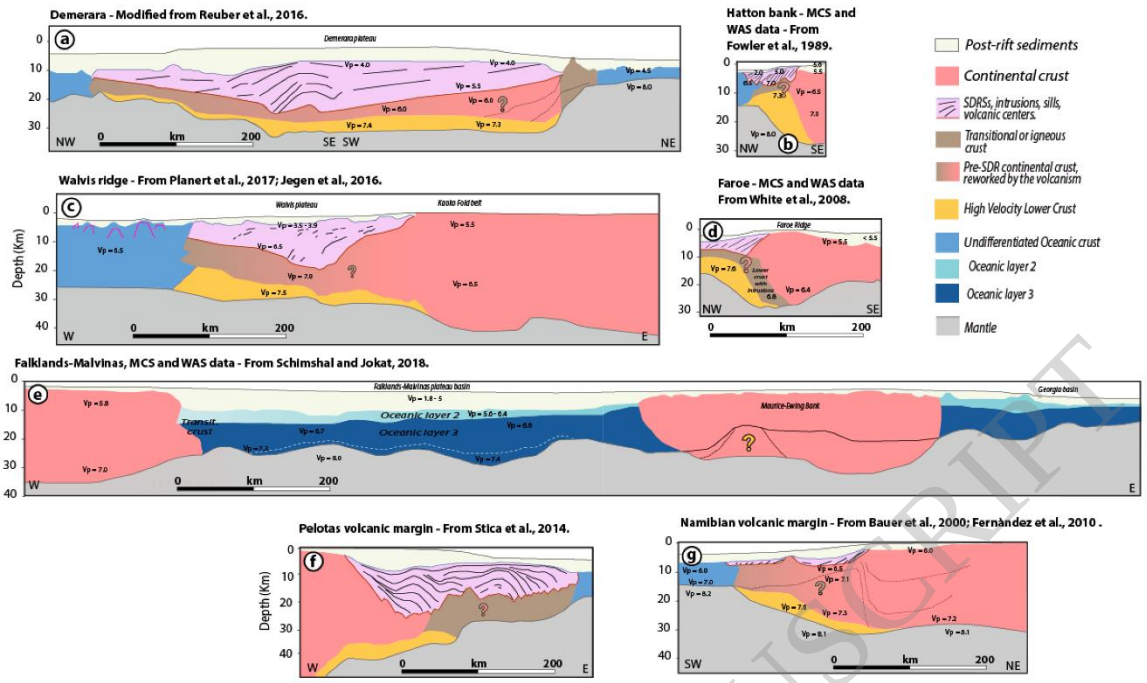

Figure 10

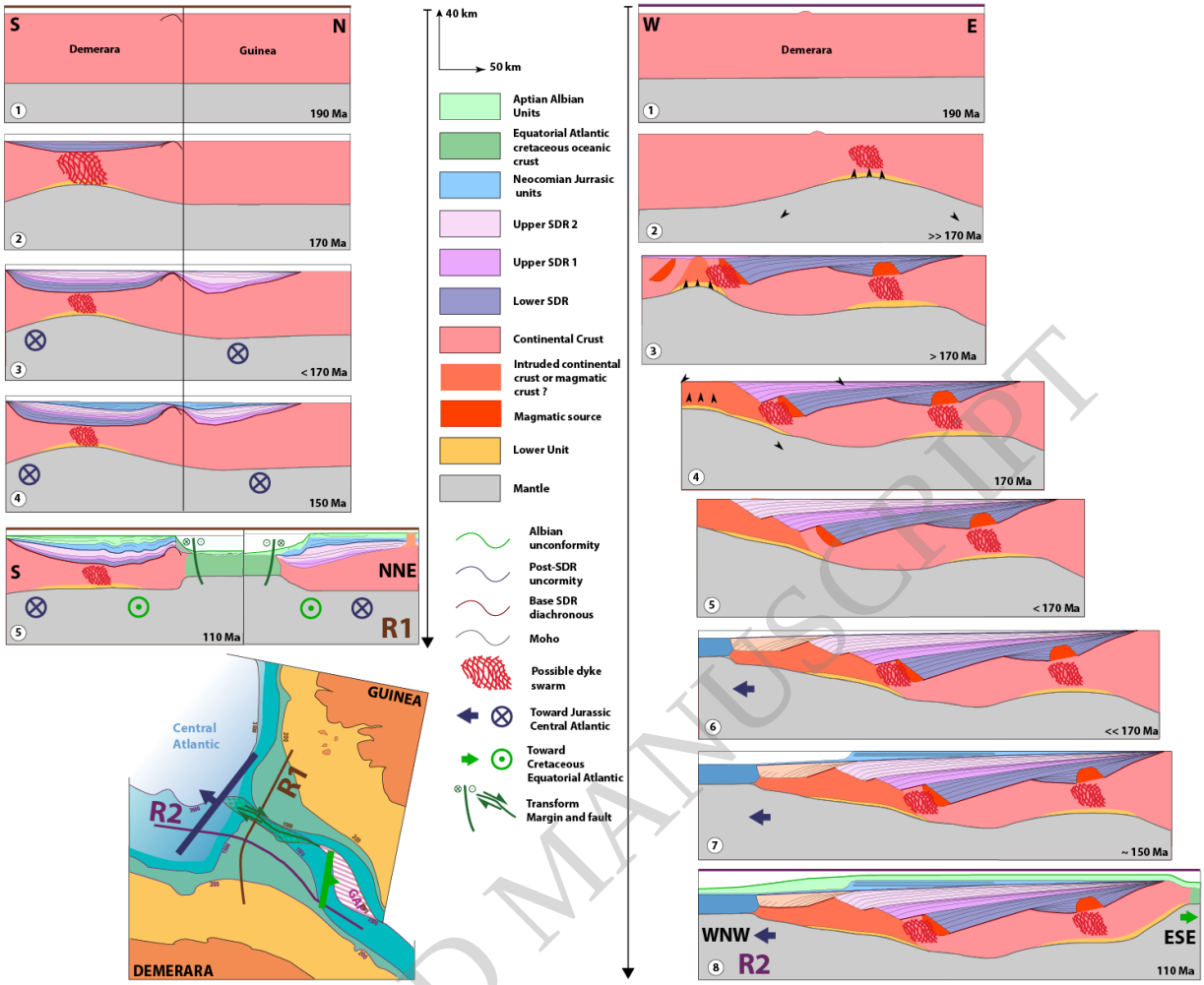

Figure 11